ALMA MATER STUDIORUM - UNIVERSITÀ DI BOLOGNA

SCUOLA DI INGEGNERIA E ARCHITETTURA

DIPARTIMENTO DI INGEGNERIA CIVILE, CHIMICA, AMBIENTALE E DEI MATERIALI

CORSO DI LAUREA IN INGEGNERIA PER L'AMBIENTE E IL TERRITORIO
Curriculum
EARTH RESOURCES ENGINEERING

TESI DI LAUREA

in
Offshore Oil & Gas Exploitation

Experimental and numerical study of methods to displace oil and water in complex pipe geometries for subsea engineering

CANDIDATO
Francesco Valentini

RELATORE:
Chiar.mo Prof. Paolo Macini

CORRELATORE
Prof. Milan Stanko, NTNU,
Trondheim

Anno Accademico 2017/18

Sessione III

Abstract

The purpose of the thesis is to study fluid displacement operations in complex pipe geometries utilized in offshore petroleum industry. Typically, Monoethylene glycol or Methanol is circulated through specific sections of the subsea production systems to lower the hydrocarbon content. This is often done at the beginning of production after a prolonged production shut-in, to avoid formation of hydrates or to minimize the emissions of chemicals to the environment when a component is to be replaced.

Experimental and numerical analyses have been conducted modifying a previously built pipe system formed like a U-shaped jumper, adding a fluid recirculation line, a jet pump, a centrifugal pump, some new valves and sensors (a flow meter and three pressure sensor). During the experiments the volume fraction in the U-shaped jumper of the displacing fluid was estimated versus time by measuring the level of the oil-water interface in each pipe segment. The system was filled and displaced with both distilled water with 3% water content of salt and Exxsol D60. Numerical simulations were performed using the one-dimensional transient multi-phase flow simulator LedaFlow. It has been investigated the necessary displacing time required to achieve target hydrocarbon concentration in the domain, optimal displacement rate for efficiently removal of hydrocarbons, and how these variables depend on two different fluids (oil and water) and their properties. The displacement has been also modelled including or removing the recirculation line.

After carrying out the simulations and performing the experiments, the results were compared, also against a new simplified mathematical model based on uniform mixing in a tank with the same volume as the pipe geometry. The results show that there is a fair agreement between the experimental results, and the results of the simplified model and the LedaFlow simulations. When including the recirculation line it took longer time to reach the target volume fraction, but the displacing rate can be lower than when the recirculation line is not present.

Preface

This Master's thesis was carried out at the Department of Geoscience and Petroleum Engineering at the Norwegian University of Science and Technology (NTNU). The thesis is written as the final part of two years Master's Programme in "Ingegneria per l'Ambiente e il Territorio", International Curriculum "Earth Resources Engineering" (ERE), with specialization in Offshore Engineering at University of Bologna, Ravenna Campus.

I would like to thank to Professor Paolo Macini, who, together with me, has always believed in this work, encouraging and helping me when necessary.

I would like to thank to Professor Sigbjørn Sangesland for giving me the opportunity to realize my Master's thesis at NTNU, and Professor Milan Stanko for supervising my work and contributing with important guidance, constantly coordinating my activity. I have always been able to rely on his valuable advices when I had doubts and problems during the preparation of my thesis.

Moreover, I would like to thank Senior Engineer Noralf Vedvik for helping me in choosing new devices to assemble, for preparing the new system configuration and for always supporting me with the system in the lab. The same gratitude is addressed to Senior Engineer Steffen Wærnes Moen for contributing with the system and the electronics when needed. I also want to thank PhD student Håvard Skjefstad for his valuable advices during the experiments I have carried in the laboratory of the Department of Geophysics and Petroleum Engineering of the Norwegian University for Science and Technology.

Bologna
Marzo 2019

Francesco Valentini

Table of Contents

List of Figure

List of Equations

List of Tables

Nomenclature

Latin Letters

A	Area [m^2]
D	Diameter [m]
f	Friction factor [-]
p	Pressure [bar]
Q	Flow rate [m^3/h] / [L/min]
U	Voltage
v	Velocity [m/s]
V	Volume [m^3] / [L]

Greek Letters

ρ	Density [Kg/m^3]
α	Volume fraction [-]
ε	Absolute roughness [m]
μ	Viscosity [Pa s]
σ	Interfacial tension [N/m]

Abbreviations

1D	One dimension
3D	Three dimension
CAD	Computer-aided design
IGP	Institutt for geovitenskap og petroleum
MEG	Monoethylene glycol
NTNU	Norwegian University of Science and Technology
P&ID	Piping and Instrumentation diagram
PVC	Polyvinyl chloride

1. Introduction

Subsea facilities are playing an increasingly important role in the creation of cost-efficient field developments. As a means to tackle both new and existing exploration and production challenges, today's oil and gas projects commonly involve a subsea concept.

It is arguably one of the most important yet technically difficult aspects of the offshore petroleum industry, but thanks to technological developments and technical expertise, subsea concepts have become a safe, mature and increasingly cost-effective option for operators looking to address both existing and new resources.

The underwater drilling and production environment presents unique challenges, particularly deep-water operations where temperature, pressure and corrosion test the durability of submerged equipment and tools.

In an offshore field, when temporarily shutting down the production of oil and gas from a well, there will still be hydrocarbons and water in parts of the subsea system such as flowlines, pipelines and manifolds.

In recent years, increasingly taking into account environmental, safety and economic factors, removal of these fluids has been taken into account, in fact constituents of produced petroleum fluids can be deposited on pipe walls when subjected to cold seawater environment. The depositions can reduce pipeline hydraulic efficiency and, in severe situations, impede flow. The quality of the fluids is strongly influenced by the characteristics of each individual site. Certain types of oils, for example, contain high concentrations of paraffin and waxes dissolved in the oil under reservoir conditions. In gas/water or gas/oil/water systems, hydrate formation is the main concern. Hydrates are compounds made up of loosely bonded light hydrocarbon (methane, ethane, and propane) and water molecules. Hydrate formation is enhanced by cold temperature, high pressure, and turbulence.

For the reasons explained above, in recent years, strong consideration has been given to removing these fluids.

One of the best options for moving the fluids that remain in the pipes is through displacement with a displacing fluid. The displacement process is conducted by injecting another fluid into the system at a certain rate; the system is circulated for a given time period that should be sufficient to remove the unwanted fluid.

Sometimes the removal of fluids in these subsea structures is not straight forward, due to uncertainties regarding displacement volumes and rates. Fluids are often displaced for a longer time period than necessary, as a consequence this turns out to be expensive. To avoid the problems listed

above, the analysis of fluid displacement in pipes is an important field to study in the oil and gas subsea engineering.

Being able to find the best combination between short time intervals to displaced fluid and a high efficiency in terms of volume fraction of the fluid displaced is therefore essential.

In the petroleum industry MEG or methanol is commonly used as displacement fluid (Opstvedt, 2016)

There has been conducted some work on the liquid-liquid flow in pipes. One of the first study was realized by Brauner (2013) that analysed and studied flow patterns and pressure drops in liquid-liquid flow. However, this study is more directed at the steady-state flow conditions in long pipes. The research at liquid displacing liquid is more limited, but it is possible to mention Schümann et al. (2014) who conducted a study on the displacement process through experiments for low flow rates with simple pipe geometries. Xu et al. (2006) conducted another interesting study, deepening about diesel oil displacing water to avoid water accumulation in low spots. He executed experiments with an inclined downhill pipe, considering also a horizontal pipe followed with diesel oil at low rates to see the displacement effect of water. Cagney et al. (2006) looked into the effect of methanol injection and gas purging to remove and inhibit water in a jumper. Dellecase et al. (2013) also studied using methanol and MEG to remove water from the geometry of a jumper.

In 2013 at NTNU Kazemihatami (2013) did his Master's thesis at NTNU on displacement of viscous oil in M-shaped jumper using water. During the work realized by Opstveld (2016), both water displaced by oil and oil displaced water were investigated in a U-shaped jumper at the IGP Department at Norwegian University for Science and Technology.

In her Master's thesis at the IGP of Norwegian University for Science and Technology also Hanne Gjerstad Folde (2017) performed an experimental and numerical study of fluid displacement in subsea pipe segments. The purpose of this study was to investigate the efficiency of one fluid displacing another fluid depending on displacement time and velocity in a U-shaped jumper. The experimental facilities are present in the laboratory of the Department of Geophysics and Petroleum Engineering at NTNU.

2. Objectives and Tasks

The topic of this Master's thesis is the "Experimental and numerical study of methods to displace oil and water in complex pipe geometries for subsea engineering". The primary objective of this work is to investigate the efficiency of one fluid given that another fluid is displaced, and considering as dependent variable the displacement time and velocity. More specifically the focus will mainly be on the study of liquid-liquid displacement in complex pipe geometries.

The study has been performed through experimental research and numerical simulations. Experiments have been carried out in a new built pipe system composed by a U-shaped jumper and a recirculation line with a new liquid jet liquid pump and a new centrifugal pump. The flushing rig is located at the laboratory hall at the Department of Geoscience and Petroleum at NTNU. In order to evaluate the displacement process tap water and the synthetic oil Exxsol D60 have been used as fluids.

In order to obtain realistic simulation models for calculating the displacement efficiency, the transient multiphase flow commercial simulator LedaFlow has been used. Moreover, the models created with LedaFlow simulator were compared to the data collected from the experiments and to the data obtained from the mathematical model, when possible.

The objectives of the project are the following:

- Planning, defining technical requirements, screen suitable components and execute modifications of the flushing rig already present in the laboratory;
- Contribute in the repair and upgrade of the experimental rig: installation of new centrifugal pump and a new jet pump, installation of the new pipes which form the recirculation line, detection and fix of leakages, general maintenance and installation of the second flow meter and pressure sensor;
- Make a three phase transient 1D numerical model using the commercial simulator LedaFlow, replacing the displacement process considering a U-shaped jumper and a new configuration that take into consideration a recirculation line, a centrifugal pump and a source, useful to simulate the jet pump;
- Validate the model created with LedaFlow, doing some experiments on the flushing rig present in the IGP laboratory, in order to compare the results.

3. Theory and Background

3.1 Subsea system

Oil and gas fields, in the quest for reserves, move further offshore into deeper water and deeper geological formations, therefore the technologies of drilling and production has advanced very sharply. The continuous increase in the use of these technologies is also due to the fact that the subsea cost is relatively flat with increasing water depth (except for the rigid platform case, for which the costs increase rapidly with water depth).

The latest subsea technologies have been proven and formed into an engineering system, namely, the subsea production system, which is associated with the overall process and all the equipment involved in drilling, field development, and field operation.

A subsea production system consists of several parts that can include a subsea completed well, a seabed wellhead, a subsea production tree, a subsea tie-in to flow line system, and subsea equipment and control facilities to operate the well. Such system can range in complexity, varying from a single satellite well with a flow line connected to a fixed platform, FPSO (Floating Production, Storage and Offloading), or onshore facilities, to several wells on a template or clustered around a manifold that transfer to a fixed or floating facility or directly to onshore facilities.

Moreover, some subsea production systems are used to extend existing platforms. For example, the geometry and depth of a reservoir may be such that a small section cannot be reached easily from the platform using conventional directional drilling techniques or horizontal wells. Based on the location of the tree installation, a subsea system can be categorized either as a dry tree production system or as a wet tree production system. Water depth can also impact subsea field development. As a matter of fact, for the shallower water depths, limitations on subsea development can result from the height of the subsea structures. Christmas trees and other structures cannot be installed in water depths of less than 30 m (100 ft). For subsea development in water depths less than 30 m (100 ft), situation in which a jacket platforms consisting of dry trees can be used.

The goal of subsea field development is to safely maximize economic gain using the most reliable, safe, and cost-effective solution available at the time.

Subsea tie-backs are becoming popular in the development of new oil and gas reserves in the 21st century. In fact, with larger oil and gas discoveries becoming less common, attention has turned to

previously untapped, and less economically viable discoveries.

Taking into account a subsea field development, the following issues should be considered:

- Deepwater or shallow-water development;
- Dry tree or wet tree;
- Stand alone or tie-back development;
- Hydraulic and chemical units;
- Subsea processing;
- Artificial lift methods;
- Facility configurations (i.e., template, well cluster, satellite wells, manifolds).

3.2 The jumper and its uses

In subsea oil and gas production systems, a subsea jumper, as it is possible to observe in figure 3.1, is a short pipe connector, either rigid or flexible, which is used to transport production fluid between two subsea components, such as a tree and a manifold, a manifold and another manifold, or for example a manifold and an export sled. It may also connect other subsea structures such as PLEM/PLETs and riser bases. In addition to being used to transport production fluid, a jumper can also be used to inject water into a well. The offset distance between the components (such as trees, flowlines, and manifolds) dictates the jumper length and characteristics. Flexible jumper systems, unlike rigid one, provide versatility, which limit space and handling capability. Usually the jumper is made up of two end connectors and a pipe between the two connectors, which may have a different shape depending on the type of jumper.

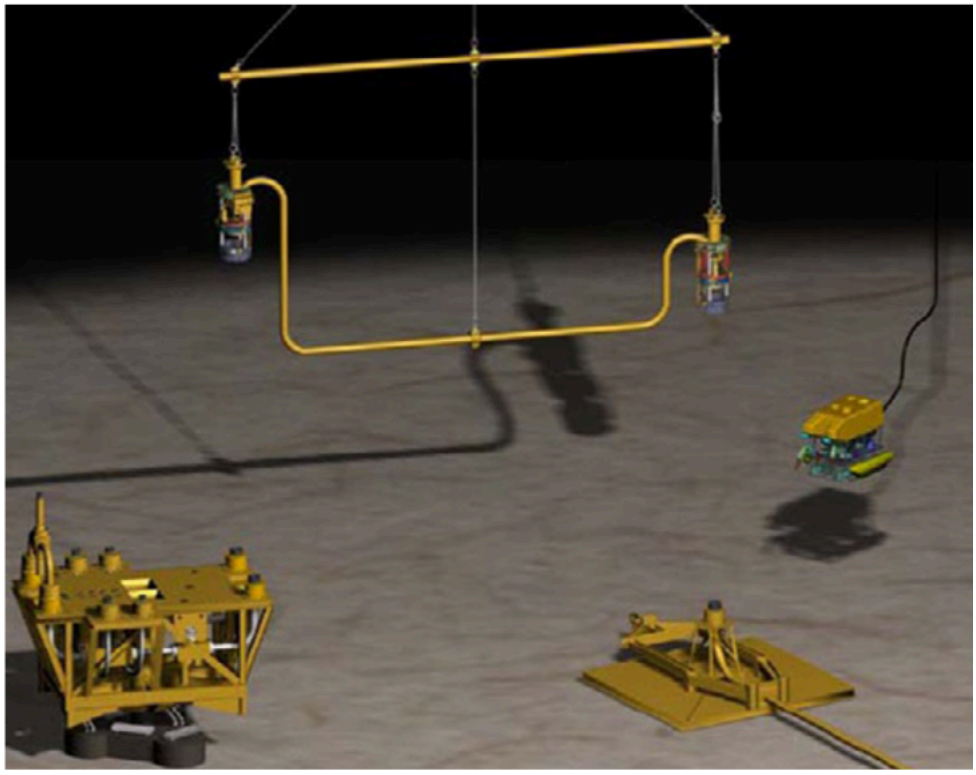

Figure 3.1: U-shaped jumper in subsea environment.

In the case under study, rigid pipes compose the jumper. The most common rigid jumper shapes are the M-shaped style and inverted U-shaped style. The subsea rigid jumpers between various components on the seabed are typically rigid steel pipes that are laid horizontally above the seabed.

After the subsea hardware is installed, the distances between the components that are to be

connected are measured. Then the connecting jumper is fabricated to the actual subsea metrology for the corresponding hub on each component, in which the pipes are fabricated to the desired length and provided with coupling hubs on the ends for the connection between the two components. Subsequently, once the jumper has been fabricated, it is transported in situ for the deployment of the subsea equipment. The jumper will be lowered to the seabed, locked onto the respective mating hubs, tested, and then commissioned.

3.3 Multiphase flow

As already mentioned above a subsea jumper is a short pipe connector used to transport a multiphase production fluid within an oil and gas production systems.

In recent years multiphase transport receives much attention within the oil and gas industry, in fact the combined transport of hydrocarbon liquids and gases, immiscible water, and sand can offer significant economic savings over the conventional platform-based separation facilities. One of the most common problems is the hydrates formation inside the pipeline that carries the fluids from the well. It is precisely for this reason that is important to consider the composition of the fluid, the increasing water content of the produced fluids, erosion, heat loss, and other factors that can create many challenges to this hydraulic design procedure.

It is possible to define a multiphase flow as a simultaneous passage in a system of a stream composed of two or more phases. Most of the time, in the oil and gas industry, multiphase flow consists of three different phases: solids, liquids and gases.

It is clear that the behaviour of a two-phase flow is much more complex than that of single-phase flow. In fact, a two-phase flow is a process involving the interaction of many variables. The gas and liquid phases normally do not travel at the same velocity in the pipeline because of the differences in density and viscosity. For an upward flow, the gas phase, which is less dense and less viscous, tends to flow at a higher velocity than the liquid phase. For a downward flow, the liquid often flows faster than the gas because of density differences.

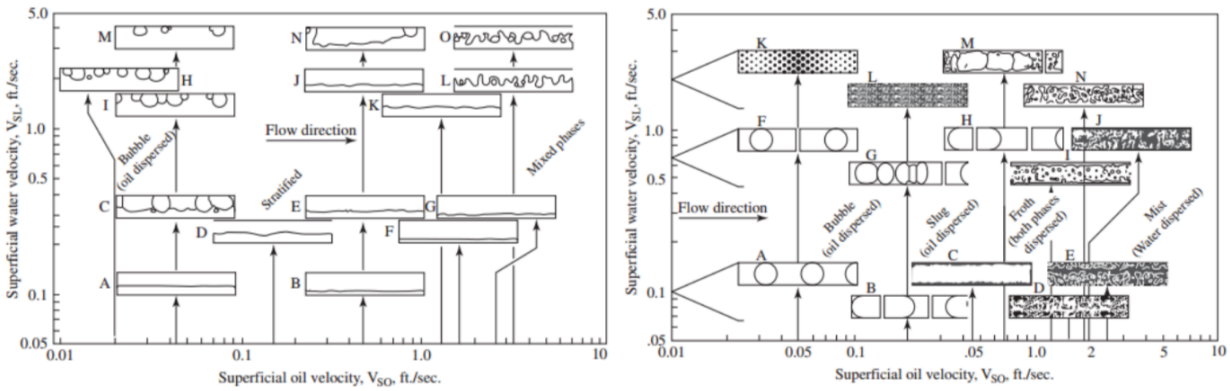

Figure 3.2: Flow pattern in case of horizontal oil – water flow (Falcone et al., 2009)

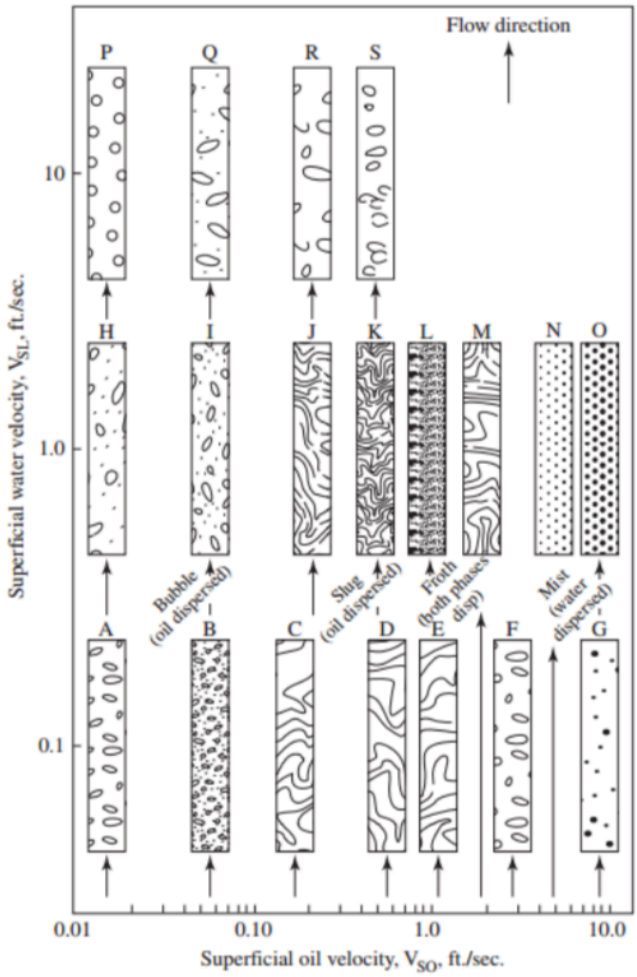

Figure 3.3: Flow pattern in case of vertical oil – water flow (Falcone et al., 2009)

However, there are some factors that may be useful to consider in to order evaluate a multiphase flow. One of the most important factors is the flow pattern, shows in figure 3.2 and 3.3. The flow pattern description is not merely an identification of laminar or turbulent flow for a single flow, since, the relative quantities of the phases and the topology of the interfaces must also be described (Y. Bai and Q.Bai). The different flow patterns are formed because of relative magnitudes of the forces that act on the fluids, such as buoyancy, turbulence, inertia, and surface tension forces, which vary with flow rates, pipe diameter, inclination angle, and the fluid properties of the phases. Transitions between flow patterns are recorded with visual technologies.

Furthermore, another important factor is liquid holdup, which is defined as the ratio of the volume of a pipe segment occupied by liquid to the volume of the pipe segment itself. Liquid holdup is a fraction that can be varies from zero, considering pure gas flow, to one for pure liquid flow.

3.4 Previously Work on Displacement at NTNU

In recent years, other experimental works have been carried out concerning the fluid displacement inside pipes. Kazemihatami (2013) conducted one of the first interesting studies about fluid displacement, and afterwards both Opstvedt (2016) and Folde (2017) wrote their Master's thesis about displacement process in jumper geometries at the Norwegian University of Science and Technology in Trondheim. A brief summary of their works and main findings will be presented in this chapter.

3.4.1 Work by Milad Kazemihatemi

Kazemihatami (2013) wrote his Master's thesis at the Department of Energy and Process Engineering analysing displacement process taking into consideration a M-shaped jumper. The experimental activities focus on investigating displacement of viscous oil in pipes by using a small scale of a jumper with an M-form, shown in Figure 3.1. The experimental setup had been designed and constructed at NTNU multiphase laboratory. Kazemihatami led a total of 56 experiments, where measurements were taken of different oil and water flows in horizontal and inclined pipelines. The results showed that the front of the shape of the propagation interface changes along the pipe, and that the minimum superficial velocity of water in order to remove all the residual oil in the jumper was 0.38 m/s.

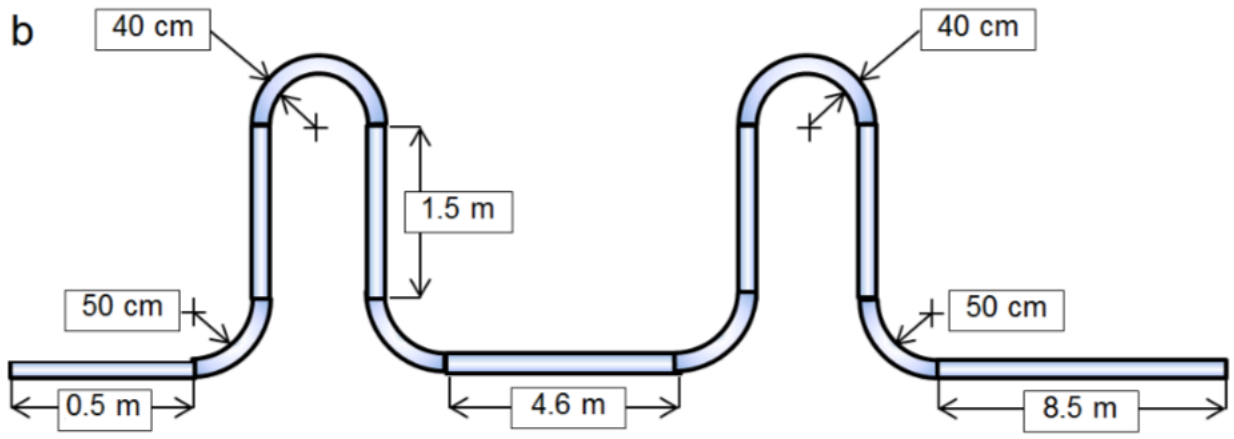

Figure 3.4: M-jumper used by Kazemihatemi during his experiments.

3.4.2 Work by Jon Arne Opstvedt

In his thesis work Opstvedt (2016) conducted an analysis in order to define how the shape of the displacement front, flow pattern and phase hold up evolve with varying displacement velocities for a jumper setup. In this case the shape of the experimental facilities was different. In fact as can be observed from the Figure 3.5 the original jumper built by Opstvedt have a U-shape, different from the one analysed in the work of Kazemihatemi (2013).

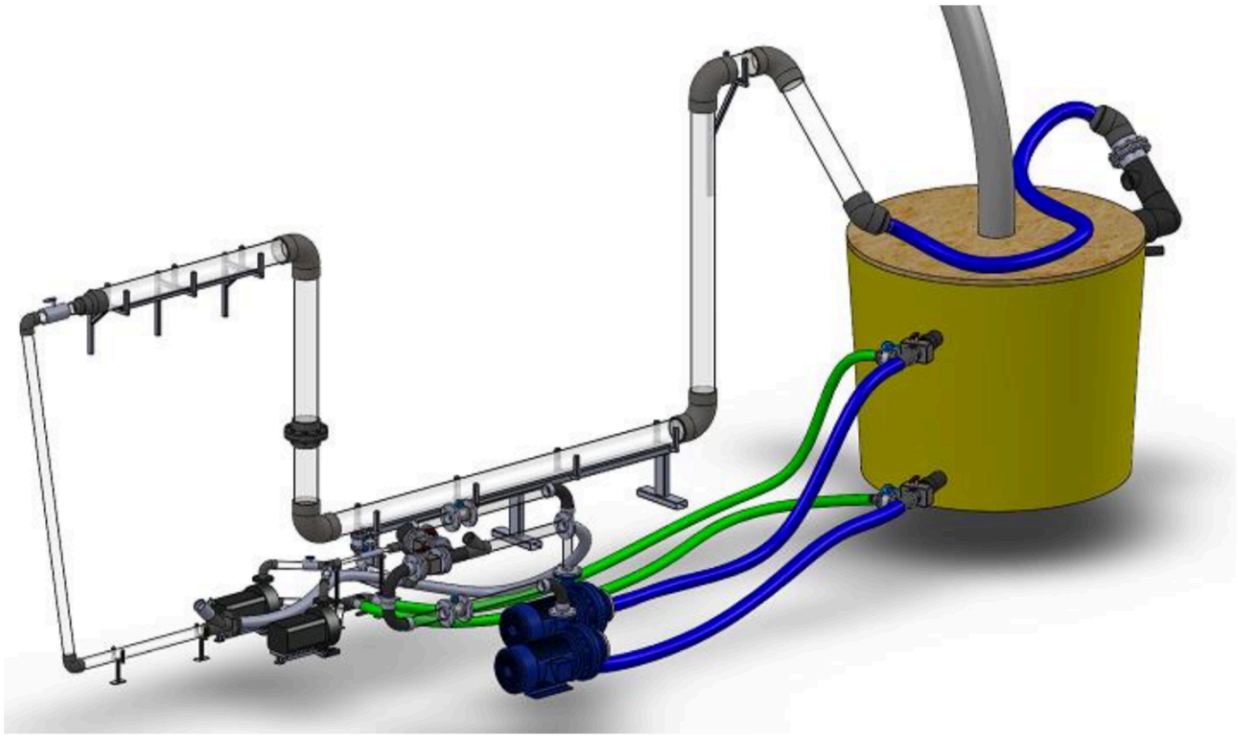

Figure 3.5: CAD of the experimental facilities created by Opstveld(2016).

During the experimentation phase, Opstvedt led a total of 16 experiments using two different geometries. Both water-oil displacement and oil-water displacement were studied for 4 different flow rates. The displacement efficiency is defined as the volume fraction of the displacing fluid at a given time. The volume fraction α of a fluid i, is calculated taking into account the ratio between total volume of fluid i in the domain, and the total volume in the domain as we can observe in the equation 3.1:

$$\alpha_i = \frac{V_i}{V_{tot}}$$

Equation 3.1: Volume fraction considering a fluid i.

According to what Opstvedt (2016) determined, the displacement efficiency is dependent on the establishment of a displacement front, which was not clearly observed until flow rates above 20

m^3/h. Analysing the results obtained in this case study it is possible to affirm that the highest displacement efficiency was seen for water-oil displacement, even though it was severely reduced after one displacement volume. Oil-water displacement showed better displacement efficiency after one volume, but with lower sweep due to reduced front height. In order to provide further detailed information regarding the multiphase flow dynamics and to examine the accuracy of the numerical model, numerical simulations were performed. Opstvedt has conducted all the simulation using the commercially available CFD software ANSYS CFX 16.2, with ANSYS workbench integration. The simulation domain was meshed using ANSYS ICEM CFD.

3.4.3 Work by Hanne Gjerstad Folde

The main goal of the thesis developed by Hanne G. Folde (2017) was to investigate the efficiency of one fluid displacing another fluid (liquid-liquid displacement) depending on displacement time and velocity.

The study was carried out through experimental research and numerical simulations. The experimental phase was performed in a previously built pipe system representing a U-shaped jumper.

The jumper is located at the laboratory hall at the IGP Department of NTNU. Two different fluids were used to conduct the experiments: tap water and the synthetic oil Exxsol D60. To obtain realistic simulation models for calculating the displacement efficiency, the transient multiphase flow commercial simulator LedaFlow was used.

During the experimental phase it was possible to observe a quick and almost linear increase in the volume fraction of the displacing fluid both for oil displacing water and for water displacing oil, until approximately one jumper volume was displaced. Moreover, it was also noted that to an increase in the flow rate of the displacing fluid correspond an increase in the displacement efficiency, where displacement efficiency is defined as the volume fraction of the displacing fluid.

In terms of flow rate, for oil displacing water, the flow rate $28.16 m^3/h \pm 1.03\ m^3/h$ was sufficient for reaching the criterion of a volume fraction of the displacing fluid above 95 %. It resulted in an oil volume fraction of 98.0 % ± 0.1 %, after 2.0 volumes displaced. On the contrary, for water displacing oil the rate $20.77 m^3/h \pm 0.67\ m^3/h$ was needed, and resulted in a water volume fraction of 98.6 % ± 0.1 %, after 2.2 volumes displaced.

3.5 Mathematical model for the definition of time and volume fraction

In order to simulate the displacement process inside the pipes a new mathematical model has been designed by professor Milan Stanko. The model has been designed to provide results of oil volume fraction in the case of a two-phase flow consisting water and oil. As will be seen below, however, the model can also be adapted to a system consisting of a three-phase flow with water, oil and gas.

The mathematical model take into account the balance between the incoming mass and the mass exiting the jumper considering a reasonable test time. The mass balance in the jumper is:

$$\frac{dm_{tot}}{dt} = \dot{m}_{in} - \dot{m}_{out}$$

Equation 3.2: Mass balance between the incoming mass and the mass exiting the jumper.

It is possible to express the total mass in the jumper as a function of the volume fractions of the different phases inside the jumper:

$$m_{tot} = m_{oil} + m_{gas} + m_{water} + m_{flushingliquid}$$

$$m_{tot} = V\,(\alpha_{oil} \cdot \rho_{oil} + \alpha_{water} \cdot \rho_{water} + \alpha_{flushingfluid} \cdot \rho_{flushingfluid})$$

The only phase that enters the jumper is the flushing liquid, at a fixed volumetric rate:

$$\dot{m} = q_{flushingliquid\_in} \cdot \rho_{flushingliquid}$$

The stream leaving the jumper has the same volumetric rate as the stream entering the jumper:

$$q_{out} = q_{flushingliquid\_in}$$

The jet pump ensures that there is good mixing of the phases inside the jumper geometry, thus the stream leaving the jumper will have the same volume fraction values as the total jumper. Whit this assumption it is possible to write the mass flow of the stream that leaves the jumper as:

$$\dot{m}_{out} = q_{flushingliquid\_in}(\alpha_{oil} \cdot \rho_{oil} + \alpha_{water} \cdot \rho_{water} + \alpha_{flushingfluid} \cdot \rho_{flushingfluid})$$

Then, substituting these expressions in the jumper mass balance equation and taking into account a case in which we have only oil and flushing liquid (e.g. water) it is possible to write:

$$\frac{d}{dt}\left(m_{oil} + m_{gas} + m_{water} + m_{flushingliquid}\right)$$
$$= q_{flushingliquid_{in}}(\rho_{flushinliquid} - \alpha_{oil} \cdot \rho_{oil} - \alpha_{water} \cdot \rho_{water} - \alpha_{gas} \cdot \rho_{gas}$$
$$- \alpha_{flushingliquid} \cdot \rho_{flushingliquid})$$

$$V \cdot (\frac{d\alpha_{oil}}{dt} \cdot \rho_{oil} + \frac{d\alpha_{water}}{dt} \cdot \rho_{water} + \frac{d\alpha_{gas}}{dt} \cdot \rho_{gas} + \frac{d\alpha_{flushingliquid}}{dt} \cdot \rho_{flushingliquid}$$
$$= q_{flushingliquid_{in}}(\rho_{flushinliquid} - \alpha_{oil} \cdot \rho_{oil} - \alpha_{water} \cdot \rho_{water} - \alpha_{gas} \cdot \rho_{gas}$$
$$- \alpha_{flushingliquid} \cdot \rho_{flushingliquid})$$

Considering that:

$$\left(\alpha_{oil} + \alpha_{water} + \alpha_{gas} + \alpha_{flushingliquid}\right) = 1$$

$$V \cdot \left(\frac{d\alpha_{oil}}{dt} \cdot \left(\rho_{oil} - \rho_{flushingliquid}\right)\right) = q_{flushingliquid_{in}} \cdot \alpha_{oil} \cdot (\rho_{flushingliquid} - \rho_{oil})$$

$$\frac{d\alpha_{oil}}{dt} = -\frac{q_{flushingliquid\_in}}{V} \cdot \alpha_{oil}$$

Separating variables it is possible to find:

$$\frac{d\alpha_{oil}}{\alpha_{oil}} = -\frac{q_{flushingliquid\_in}}{V} \cdot dt$$

Integrating between initial condition and time "t" it is possible to find the a-dimensional value of the oil volume fraction with the equations:

$$\ln(\alpha_{oil})_{\alpha_{oil}(t=t_0)}^{\alpha_{oil}(t)} = -\frac{q_{flushingliquid\_in}}{V} \cdot (t - t_0)$$

$$\alpha_{oil} = \alpha_{oil\_initial} \cdot e^{-\frac{q_{flushingliquid_{in}}}{V} \cdot (t - t_0)}$$

Equation 3.3: Oil volume fraction.

By imposing some different value of flow rate ($q_{flushingliquid}$) the time to have an oil volume fraction less than 10% was determined and the results are show in the following table.

Flow rate	Time	Oil volume fraction	Water volume fraction
m^3/h	s	[-]	[-]
2	960	0,09938	0,90062
3	640	0,09938	0,90062
5	384	0,09938	0,90062
8	240	0,09938	0,90062
10	192	0,09938	0,90062
13	148	0,0989	0,9011
15	128	0,09938	0,90062
18	108	0,09655	0,90345
20,77	96	0,09096	0,90904

Table 3.1: Volume fraction results of mathematical model

From the results presented in the table and from the figure 3.3 it is possible to state that, by increasing the speed, the displacement time necessary to reach a value of less than 10% of oil volume fraction decreases. In particular, figure 3.6 shows the oil volume fraction evolution for different imposed value of flow rate with time. The displacement efficiency is defined as the volume fraction of the displacing fluid at a given time.

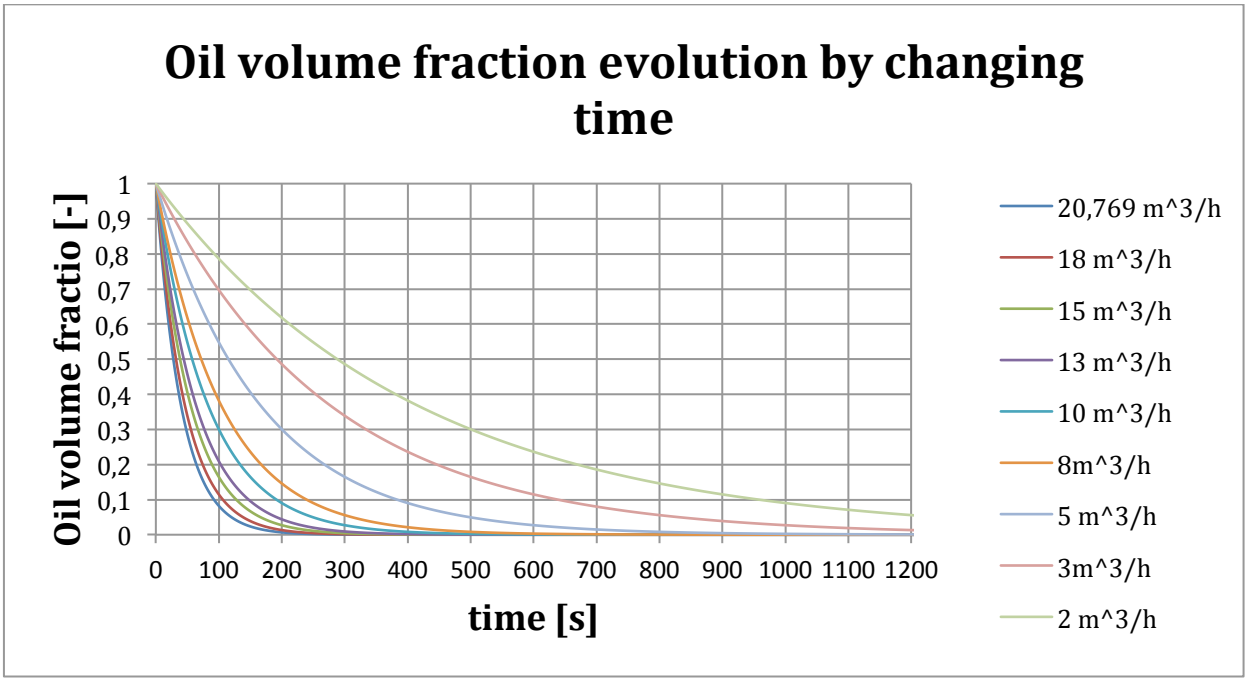

Figure 3.6: Oil volume fraction evolution by changing time.

3.6 Numerical Analysis

To simulate the movement of a multi-phase fluid, there are several commercial software available on the market. One may choose between the 1D simulator tools LedaFlow by KONGSBERG and OLGA by Schlumberger, or the 3D computational fluid dynamic tool ANSYS CFX. LedaFlow is a transient multiphase flow simulator, based on multiphase physics from large-scale experiments and gathered field data. Transient simulation with the OLGA simulator provides an added dimension to steady-state analyses by predicting system dynamics such as time-varying changes in flow rates, fluid compositions, temperature, solids depositions and operational changes.
The CFD software is governed by physical laws, and applied through averaged Navier-Stokes equations along with models for phase interaction and turbulence (Opstvedt, 2016). In the present work, LedaFlow will be explored as a tool for simulating displacement, and compared to the models made with the same simulator by Folde 2017.

3.6.1 LedaFlow simulator

LedaFlow is the product of ten years of innovative development by SINTEF sponsored, guided and supported by important sector leader such as TOTAL and ConocoPhillips. This software is marketed and developed further by KONGSBERG.

LedaFlow is based on models that are closer to the actual physics of multiphase flow and provides a step change in detail, accuracy and flexibility over existing multiphase flow simulation technology. The software has been validated against the best available and most comprehensive experimental data sets to ensure that the models are as best representative as possible and is designed with an user interface, which is easier and more intuitive to use.

Two models are included in LedaFlow: the Point model and the 1D model.

The Point model is used for “one point” of all the three flow cases; single, 2-phase (liquid and gas) and 3-phase to solve steady state equations. It is assumed that there exists a thermodynamic equilibrium, which means no compositional effects are taken into account when the fluid distribution is computed. The mixture temperature is giving the foundation of the temperature distribution. In the Point model a fast and steady state solution with exact mass conversion is reached, and is the basis of the steady-state pre-processor for 1D transient code.

The other model, 1D model, is used for transient situations for the same three flow cases. In the field approach from LedaFlow there is included a detailed modelling of water and oil dispersions

and gas bubbles in liquid phase, where there exists a mass equation for each field. The fields are visualized in Figure 3.7.

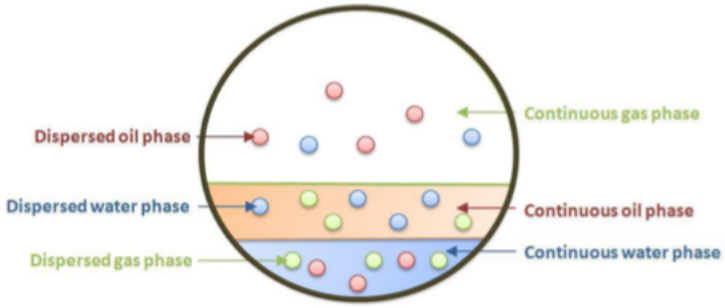

Figure 3.7: Fields used in the 1D model in LedaFlow.

The equations for enthalpy and energy are solved for continuous phases. In this model, heat transfer and complex networks with manifolds, wells, valves, controllers, etc. are included. (KONGSBERG, 2016b).

4. Experimental facilities

This chapter first describes the type of fluids used for the realization of the simulations phase (made by LedaFlow simulator) and experiments in the laboratory. After this part there is a description of the previous configuration of the flushing rig and a description of the new configuration, which is the subject of study of this master's thesis. The last part is about the creation of numerical models in LedaFlow.

4.1 Hydraulic pressure model

In order to understand and predict the possible pressure losses inside the pipe system can be, a model has been created. The starting flow rate is 13m^3/h.

The model has been created for 3 different configurations: a first configuration in which the jumper is completely filled with oil, in this phase the maximum oil volume fraction and a fraction equal to 0 of water was considered (the density and viscosity of the oil have been taken into consideration), an intermediate configuration during which the displacement process is underway and so the water volume fraction and the oil volume fraction are considered the same, and a third phase in which the water almost completely displaced oil, therefore it is possible to find a high value of water volume fraction and a very low quantity of oil inside the jumper.

	Starting conditions	Transitional conditions	Final conditions
Water volume fraction [-]	0	0,5	0,902
Oil volume fraction [-]	1	0,5	0,098
Water density Kg/m^3	998,9	998,9	998,9
Oil (ExxolD60) density Kg/m^3	786	786	786
Total density kg/m^3	786,00	892,45	978,04
Viscosity Pa s	0,00156	0,00133	0,001095

Table 4.1: Conditions reproduced in the model

A fluid flowing inside a pipe is subject to the so-called distributed pressure losses, a pressure drop due to the internal friction. A fundamental parameter for the definition of pressure losses is the friction coefficient, in this circumstance determined with the Haaland formula.
Professor S.E. Haaland of the Norwegian Institute of Technology (NTNU) proposed the Haaland equation in 1983. It is used to solve explicitly for the Darcy-Weisbach friction factor *f* for a full-

flowing circular pipe. It is an approximation of the implicit Colebrook–White equation, but the discrepancy from experimental data is well within the accuracy of the data.
The Haaland Formula is:

$$\frac{1}{\sqrt{f}} = -1{,}8\ log\left[\left(\frac{\frac{\epsilon}{D}}{3{,}7}\right)^{1{,}11} + \frac{6{,}9}{Re}\right]$$

Equation 4.1: Haaland equation to determine friction factor.

In the previous equation "Re" is the Reynolds number determined by the equation:

$$Re = \frac{vD\rho}{\mu}$$

Equation 4.2: Reynolds number.

The result of the calculation useful to determine the friction factor are expressed in the table below:

Friction factor - Haaland equation			
Roughness (m)	Diameter (m)	Re	Friction factor
0,0000015	0,153	26854,7	0,3934
0,0000015	0,16	25679,8	0,3944

Table 4.2: Friction factor based on diameter and Reynolds number

The distributed pressure losses have been determined with the formula:

$$\Delta P = f\frac{L}{D}\frac{v^2}{2}\rho$$

Equation 4.3: Distributed hydraulic pressure losses.

Where:

- f is the friction factor determined with Haaland Equation.
- L is the length of the pipe expressed in meters;
- D is the diameter of the pipe expressed in meters;
- v is the velocity determined by the ratio of the imposed flow rate (m^3/h) and the area of the pipes (m^2).
- ρ is the density of the fluid expressed in Kg/m^3.

In the event that the fundamental cause of dissipation is given by the geometric configuration or the presence of any accidentality, such as bends, elbows, valves, faucets, we will have pressure losses called concentrated. This denomination depends on the fact that they are located in precise points of the conduit and not distributed along the entire length of the tube.

In the experimental facilities there are also elbows and it is therefore important to determine the concentrated pressure losses.

The formula employed is:

$$\Delta P = \beta \frac{v^2}{2} \rho$$

Equation 4.4: Concentrated pressure losses.

The term β, which correspond to the friction coefficient, depends on the particular geometry of the object that determines the loss, and is tabulated. In the event of a loss due to the presence of a 90° elbow the value of β is equal to 0,9 and it is dimensionless.

	Length of the pipes (m)	Diameter (m)	Re	Friction factor	ΔP (bar)
Section 1	1	0,153	26854,7	0,3934	0,0005
Elbow 1		0,16	25679,8	0,3945	0,0001
Section 2	1,6	0,153	26854,7	0,3934	0,0008
Elbow 2		0,16	25679,8	0,3945	0,0001
Section 3	1,536	0,153	26854,7	0,3934	0,0007
Elbow 3		0,16	25679,8	0,3945	0,0001
Section 4	1,5	0,153	26854,7	0,3934	0,0007
Elbow 4		0,16	25679,8	0,3945	0,0001
Section 5	3	0,153	26854,7	0,3934	0,0015
Elbow 5		0,16	25679,8	0,3945	0,0001
Section 6	2	0,153	26854,7	0,3934	0,0010
Elbow 6		0,16	25679,8	0,3945	0,0001
Section 7	0,3	0,153	26854,7	0,3934	0,0001
Elbow 7		0,16	25679,8	0,3945	0,0001
Section 8	2,1	0,153	26854,7	0,3934	0,0010
Elbow 8		0,16	25679,8	0,3945	0,0001
Section 9	1	0,153	26854,7	0,3934	0,0005
Total ΔP					**0,0080**

Table 4.3: Total pressure losses in the U-shaped jumper

Observing the values included in the table 4.3 it is possible to state that the total pressure drops are very low, due above all to the friction of the fluid on the walls of the pipes and to the losses concentrated in the elbows.

4.2 Fluids

Both for the simulation phase with LedaFlow simulator and for the following experimentation phase in the laboratory, tap water and oil Exxol D60 (produced by ExxonMobil Chemicals) were used.

During the testing phase, to reduce the possibility of errors due to changes in the intrinsic properties of the fluids used, the characteristic parameters of tap water and oil Exxsol D60 have to be the same. In this case the properties of the oil remain unchanged, while the properties of water can change day by day or may vary from place to place. Since the experiments were carried out in a single week, it can be assumed that the properties of the water remain unchanged.

Certainly it would have been better to use crude oil in order to simulate a closer case-study to a real situation of deposit, but due to the fact that it is not easy to find this material on the market, and take into account its toxicity, Exxol D60 oil was used. In fact, this product has values similar inherent characteristics parameters comparable with real ones.

Exxsol D60 Fluid is produced from petroleum-based raw materials, which are treated with hydrogen in the presence of a catalyst to produce a low odour, low aromatic hydrocarbon solvent. The major components of this product include normal paraffin, isoparaffins, and cycloparaffins.

Reading the product specifications from ExxonMobil (2005) one can see that the viscosity at 25 °C is 1.43 mPa s. Due to high temperatures, real crude oils might actually exhibit viscosities similar to the Exxsol D60. The interfacial tension between water and Exxsol D60 has been measured to 36 mN/m in 2016 by SINTEF, using a Pendant Drop measurement method with a Teclis Tracker tension meter from Teclis Instruments (Fossen, 2016).

Exxsol D60 Fluid is generally recognized to have low acute and chronic toxicity. Vapour or aerosol concentrations above the exposure limit of 184 parts per million (ppm) in the air can cause eye and lung irritation and may cause headaches, dizziness or drowsiness. Prolonged or repeated skin contact in an occupational setting may result in irritation so for this reason, during the laboratories activity, all appropriate security measures have always been used (use of chemical resistant gloves and glasses is recommended). Exxsol D60 fluid is not regarded as a mutagen or carcinogen, and there is low concern for reproductive, developmental, or nervous system toxic effects.

In order to distinguish between the transparent liquids, Exxsol D60 and water, the oil was dyed with “Oil Red O” color powder. The Oil Red O color powder does not affect the surface tension of the oil (Chen et al., 2016).

4.3 Configuration of experimental facilities

This chapter makes an excursus explaining the previous configuration and all the changes that have been made to it to arrive at a new configuration of the flushing rig. Below we will deepen the characteristics of the new devices that have been purchased and mounted on the new flushing rig. The characteristics of the new jet pump are also described below. In order to purchase the best product according to our technical requirements, a model has been created specifically for this case study. In detail below the characteristics of the flow meters and pressure sensors installed in the new model of flushing rig were described.

4.3.1 Previous Configuration

The previous configuration of the U-shaped jumper used by H. Folde (2017) in her thesis is the same as built by Opstvedt (2016).

As can be seen from the figure 4.1 the jumper consists of several parts: a horizontal inlet, a vertical pipe, a horizontal bottom pipe and a second vertical pipe. The fluid leaving the jumper is conveyed to the separator.

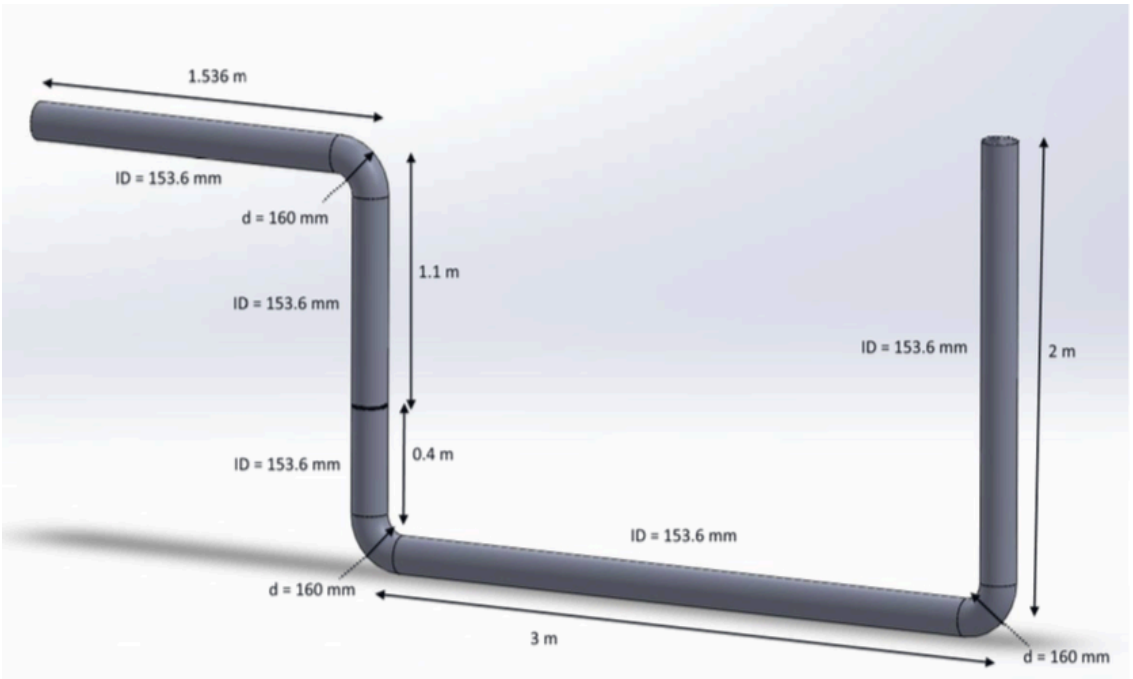

Figure 4.1: Measures of the U-shaped jumper based on Opstveld (2016)

The U-jumper designed and built by Opstvedt (2016) has two configurations. The first geometry is the regular one, made using the first horizontal pipeline at the top as the inlet and inserting a blind

flange in the first riser, as shown in Figure 4.2 (Opstvedt, 2016). Then the whole volume of the jumper is investigated.

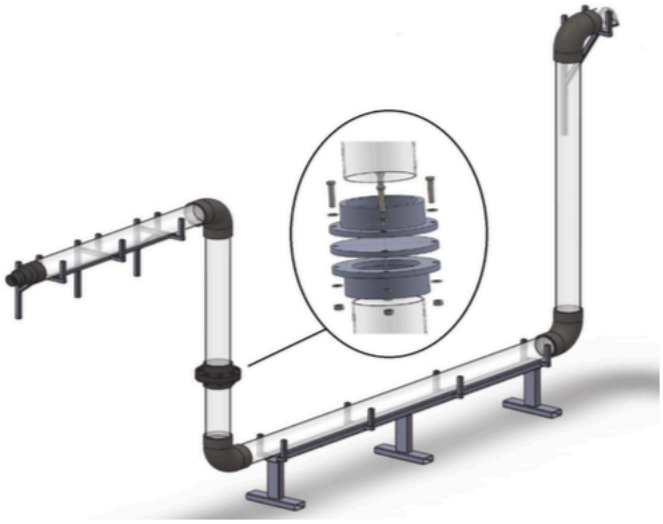

Figure 4.2: U-jumper with blind flange in the first riser (Opstvedt, 2016)

Unlike the first, for the second geometry an extra inlet is built, shown as the bottom inlet in Figure 4.3 (Opstvedt, 2016). When the first riser is cut off, this gives the possibility of studying displacement in a closed off section.

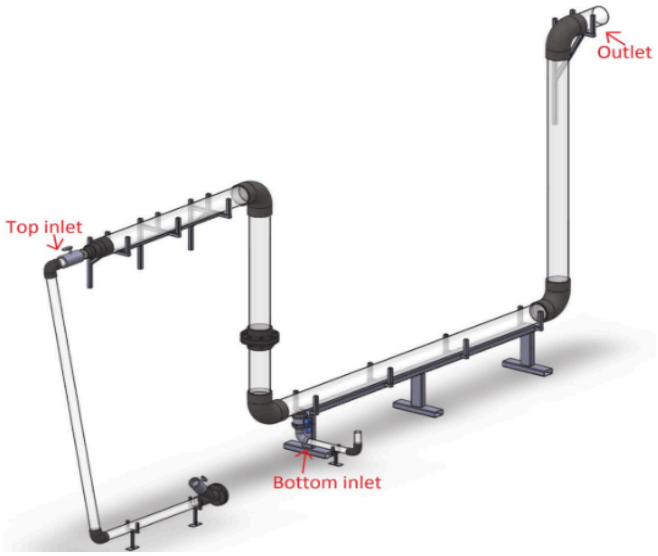

Figure 4.3: U-jumper with the bottom inlet and outlet of the jumper (Opstvedt, 2016)

It was requested that all of the pumps should have the possibility of being used for the three different experiment facilities, both in pairs or separately. This required a flexible system for the pumps. A manifold was designed by Senior Engineer Noralf Vedvik at NTNU to combine the pumps, and the design of the system is shown in Figure 4.4.

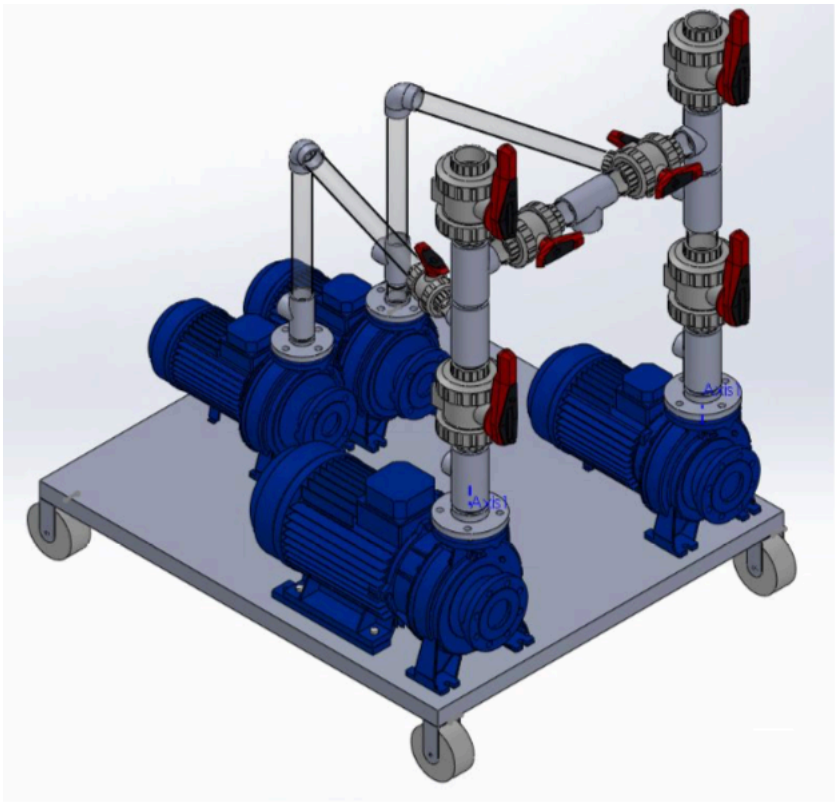

Figure 4.4: Manifold for pumps (Drawing by Espen Hestdahl)

In the figure 4.5 it is possible to observe a piping and instrumentation diagram of the previous configuration that include valves, pumps, pipelines, separator, the flow meter (marked with an F) and all the pressure and temperature sensors that are located in different part of the flushing rig.

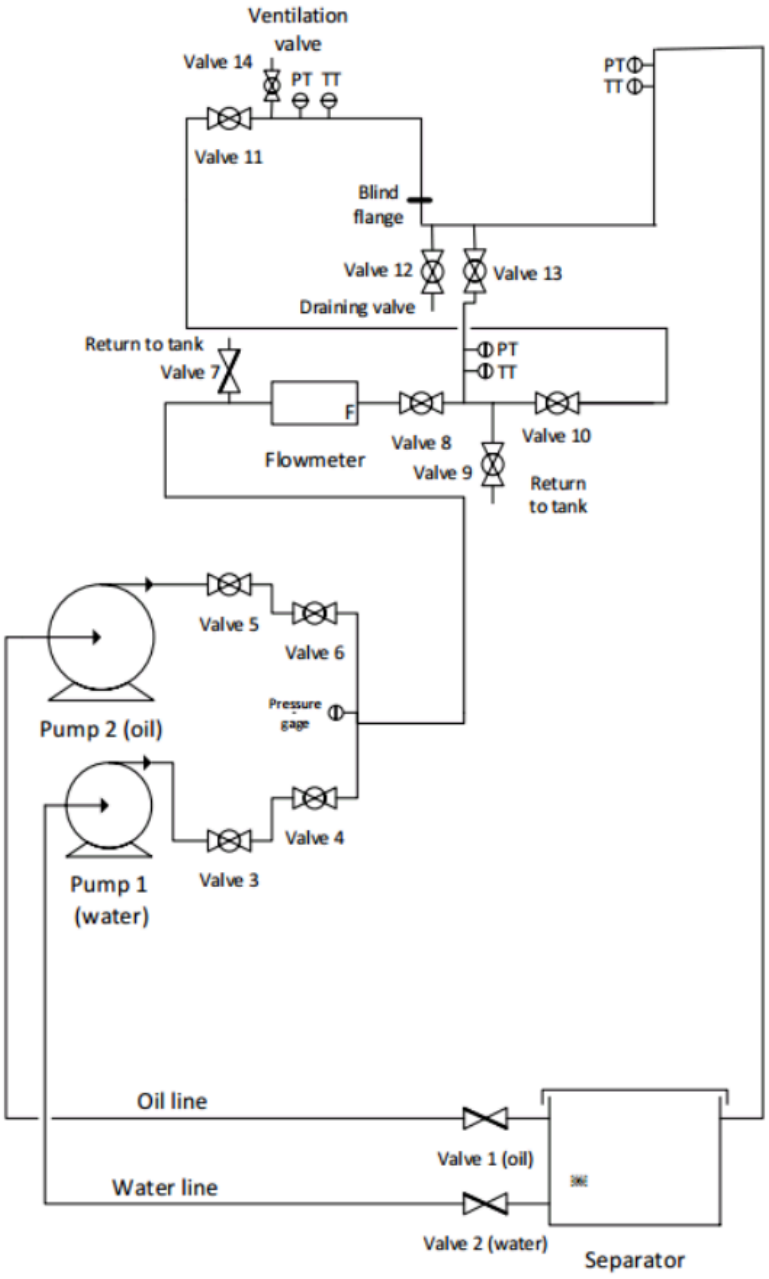

Figure 4.5: P&ID of the previous configuration (Folde 2017)

4.3.2 A new configuration

The idea of a new layout of the flushing rig was conceived in order to improve its efficiency, reducing the time needed to displace one fluid with another. To better explain all the differences between the previous configuration and all the changes made for the realization of the new configuration of the flushing rig, a 3D model was created, using the software Rhinoceros.

Compared to the previous configuration, as it is possible to observe from the figure 4.6, a new fluid recirculation line, another flow meter, a new jet pump, and a new centrifugal pump was added. In this case the fluid drainage points are three, one located in the lower part of the jumper and the other two positioned respectively before and after the jet pump.

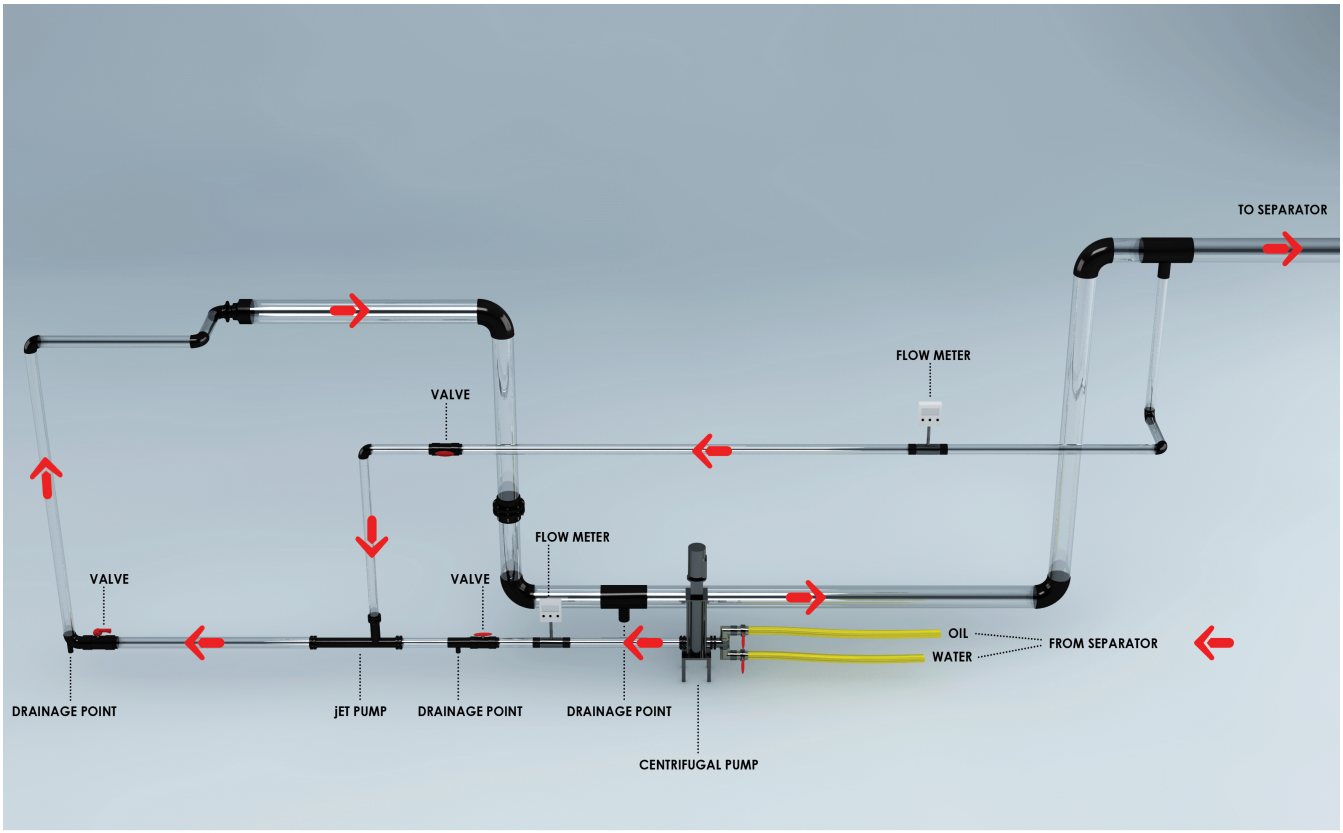

Figure 4.6: Sketch of the new configuration of the flushing rig.

The red arrows in the figure 4.6 indicate the flowing direction of the liquid inside the flushing rig during the experimental phases.

The new flow meter has been positioned in the new fluid recirculation line, also to measure the flow rate to the jet pump and to evaluate its usefulness and efficiency.

The new centrifugal pump is a vertical, multistage pump with suction and discharge ports at the same level (in-line) enabling installation in a horizontal one-pipe system. The pump is fitted with a 3-phase, fan-cooled, permanent magnet, synchronous motor. The motor includes a frequency converter and PI controller in the motor terminal box. This enables continuously variable control of the motor speed, which again enables adaptation of the performance to a given requirement.
In the experiments, all pipes in the figure were filled initially with the fluid to be displaced with the aid of the centrifugal pump that draws the liquid directly from the separator. After that, the pump was turned off and the valves in the pump suction manifold were closed and open to select the source of the displacing fluid (if, for example, the tube was filled with oil the oil valve was closed and the valve opened allowing water to flow into the system).

The injected flow rate has been set manually, adjusting the valve opening positioned immediately after the flow meter (the valve is indicated with an arrow in the figure 4.7) and adjusting the power of the centrifugal pump. The valve was opened or closed until the flow meter indicated the desired flow rate.

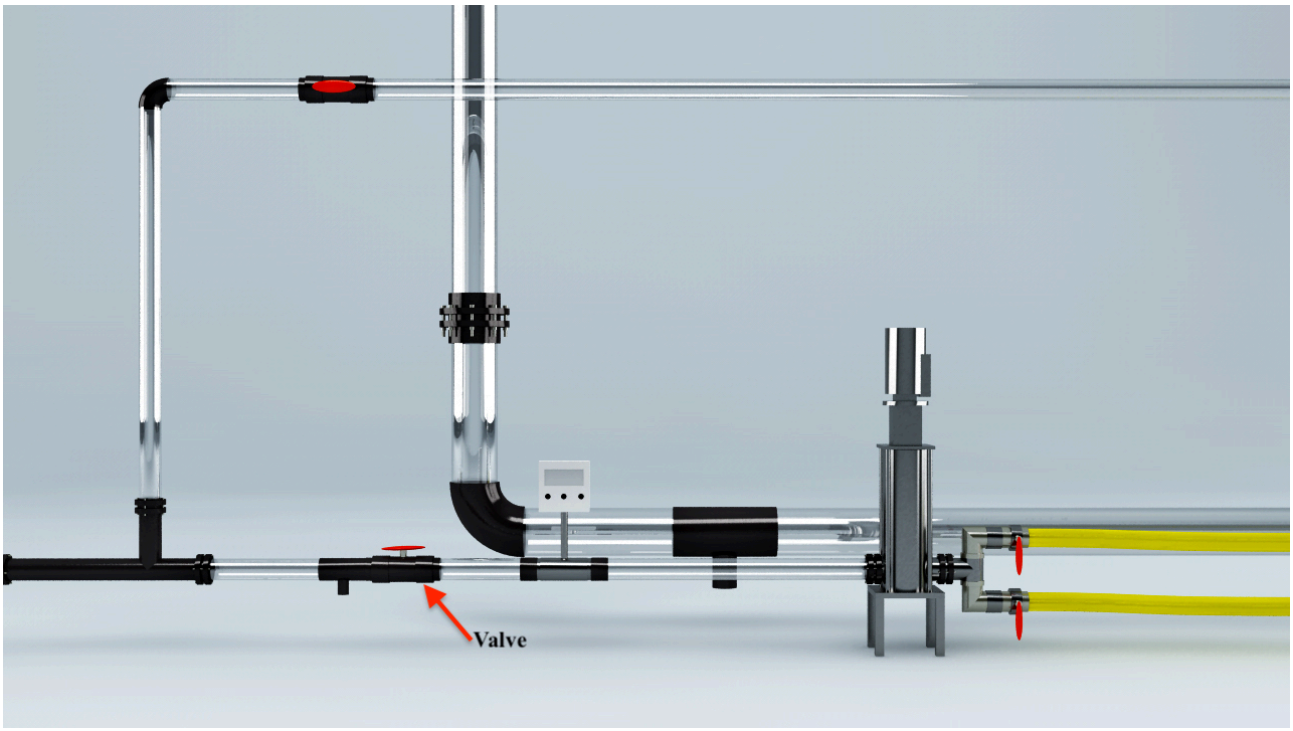

Figure 4.7: Detail view of the new configuration of the flushing rig.

Figure 4.8: Lateral view of the new configuration of the flushing rig.

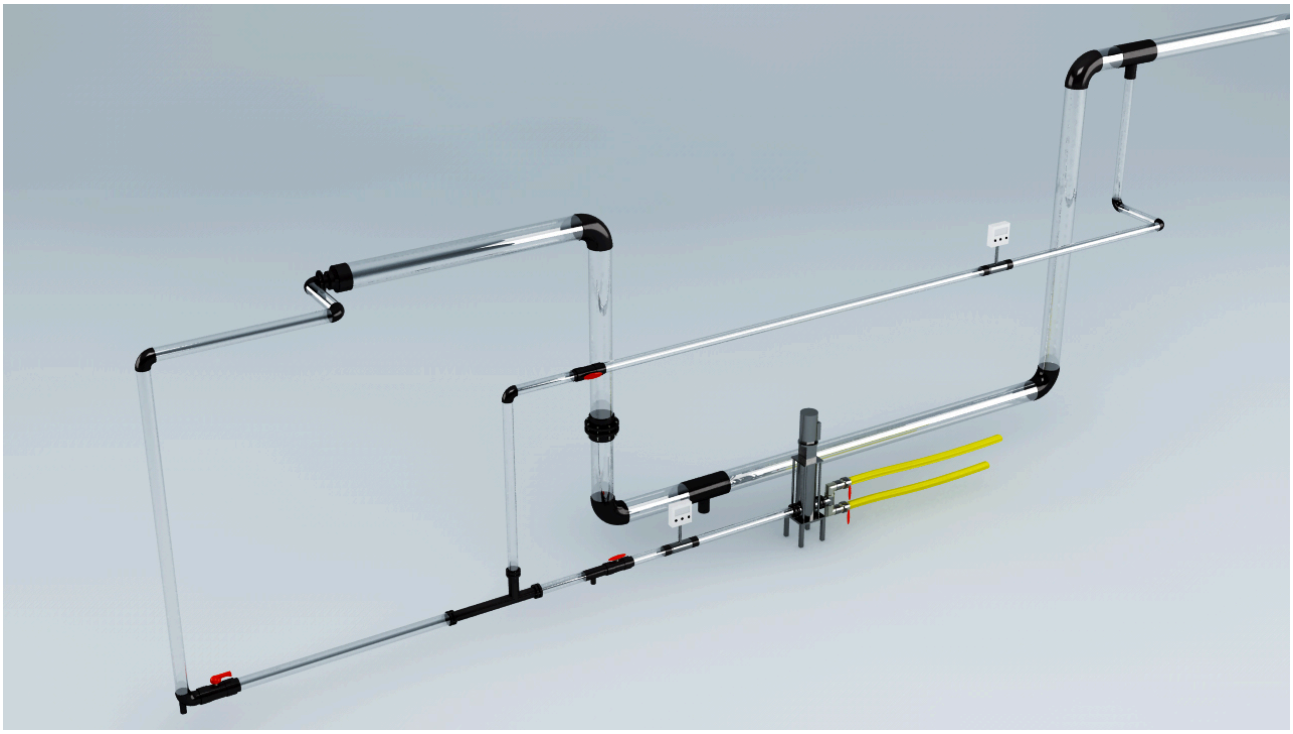

Figure 4.9: Top view of the new configuration of the flushing rig.

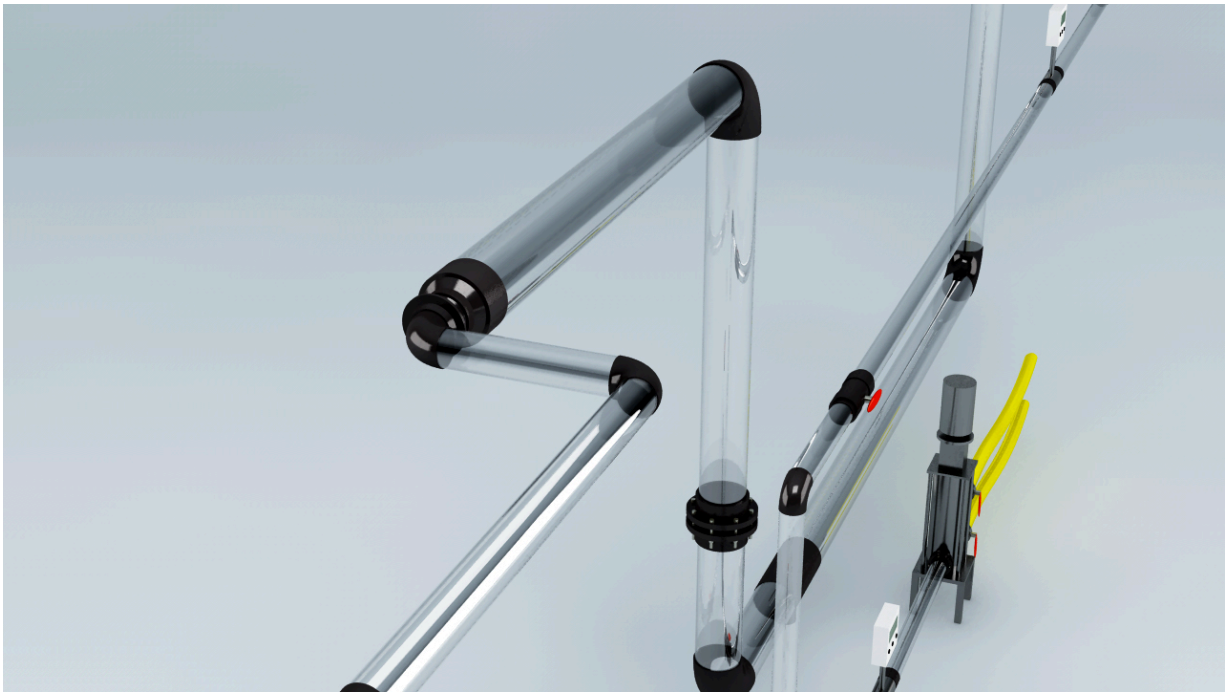

Figure 4.10: Top view of the new configuration of the flushing rig.

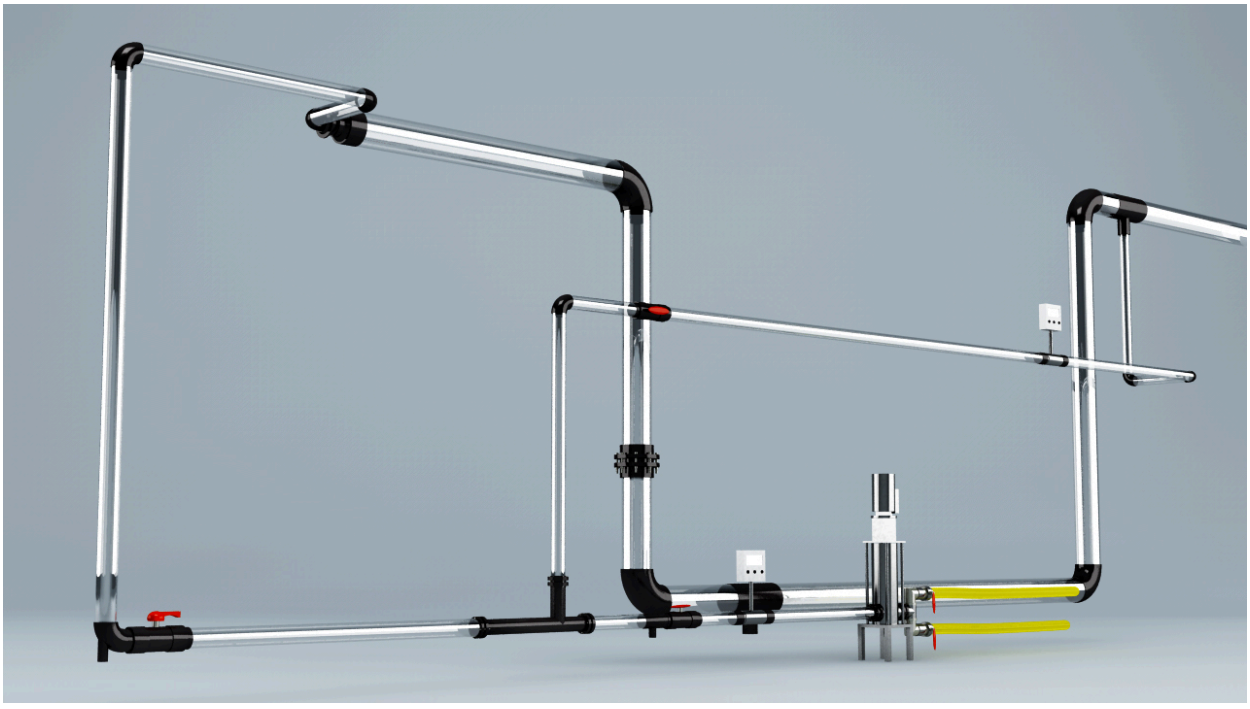

Figure 4.11: General view of the new configuration of the flushing rigs.

4.4 Jet Liquid Jet Pump

The ejectors are equipment designed to use the energy made available by a high-pressure fluid to boost the pressure of a low-pressure stream. They can provide the use of compressible fluids or incompressible fluids, being able to work also with fluids of different nature. Considering the figure 4.12, it is possible to state that ejector are composed of three most important parts, which are always present and do not depend on the nature of the fluids used:

- The nozzle, which injects the high pressure fluid into the groove section of the mixing pipe;
- The mixing chamber, where the two fluids are mixed;
- The diffuser, which allows the fluid to escape from the pump, able to converts the kinetic energy of the outlet flow into pressure energy thus performing the useful effect of fluid compression;

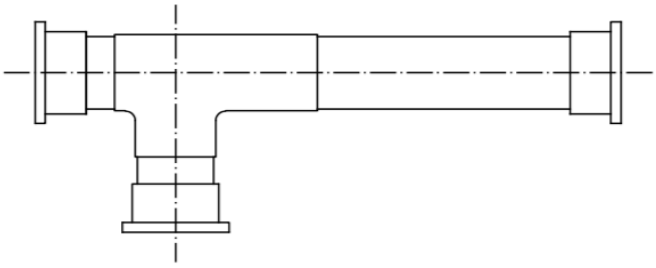

Figure 4.12: Jet pump sketch

The high-pressure motor fluid (or primary fluid) is passed through a nozzle where its pressure energy is converted into kinetic energy. By positioning the nozzle on the throat section of a convergent-divergent conduit, the high-speed flow succeeds in sucking the low-pressure fluid (suction fluid or secondary fluid) into the conduit. The two flows are then mixed together in the mixing chamber, which allows an initial pressure increase. A further pressure recovery occurs when the flow passes through the diffuser positioned immediately after the mixing chamber before leaving the machine.

The operating characteristics of an ejector depend on the temperature and molar mass of the working fluids. The greater the molar mass of the fluid the greater the suction capacity of the ejector, assuming constant the flow rates of the motor fluid. Parallel to the molar mass a reduction of the suction capacity is obtained with the increase of the fluid temperature.

The operating principle of an ejector is based on the operation of the Venturi tube. The Venturi effect is the physical phenomenon where the pressure of a fluid current increases with decreasing speed. Considering a conduit having a reduction of the section inside, run by a fluid with constant density, so taking into account an incompressible fluid, from the equation of continuity in stationary conditions, the mass flow entering the major section must be equal to that entering the minor section. Considering these assumptions, the volumetric flow rate can be expressed as a product of the speed for the passage section.

$$A_1 \times v_1 = A_2 \times v_2$$

From this relationship it is deduced that a reduction in the section corresponds to an increase in speed.

Through the Bernoulli equation:

$$\rho g h_1 + p_1 + \frac{1}{2}\rho v_1^2 = \rho g h_2 + p_2 + \frac{1}{2}\rho v_2^2$$

Assuming that there is no difference in height between the two sections considered, the following equation is obtained:

$$p + \frac{1}{2}\rho v^2 = cost$$

As a consequence of the previous steps is possible to obtain a correlation between the pressure and the velocity in a given section; it is possible to state that the velocity of the fluid increases, the internal pressure of the fluid itself is necessarily reduced to maintain its constant sum.

This type of pump never has high efficiency, generally never higher than 30%. The constructive simplicity and the absence of moving parts inside them allows a good economy in particular contexts, for example where there is an availability of high pressure fluids or in cases where it is located in places that are not easily accessible and is difficult to access for routine and extraordinary maintenance.

The main advantages deriving from the use of ejectors reside in a high constructive reliability not having moving parts inside them, in the low initial investment costs and minimum operability costs following installation, thanks to the absence of lubrication systems sometimes necessary with the use of compressors. The installation of ejectors brings with it a reduction in the level of vibrations during operation and a drastic reduction in terms of costs.

4.5 Jet pump model for the case study

The jet liquid jet pump was not present among the instruments owned by the laboratory and it was therefore necessary to purchase a new one. In order to choose the correct type of jet pump with the best performance in relation to our case study, a model able to simulate conditions similar to those reproducible in the laboratory during the tests was created. The model is based on some important assumptions:

- The model is based on the one-dimensional theory.
- The primary and secondary flows enter the mixing throat with uniform velocity distribution, and the mixed flow leaves the diffuser with uniform velocity distribution.
- The fluid in the primary and secondary flows is the same.
- The fluid is assumed to be incompressible and containing no gas.
- The primary flow rate (q_1) is always the same.

The model has been created for different injected flow rates, always considering a fixed primary flow rate of about 8 m^3/h and changing the secondary flow rate until a maximum total discharge flow rate of 23 m^3/h is reached.

Particular attention has been paid to the case where the flow rate is maximum (23 m^3/h). Considering that the primary flow rate, which correspond to the q_1 in the figure 4.13, is fixed at 8 m^3/h, it is possible assume that the secondary flow rate, q_2 in the figure 4.13, is equal to 15 m^3/h. Knowing the input diameter for the primary and secondary flow rate, the input velocity were determined.

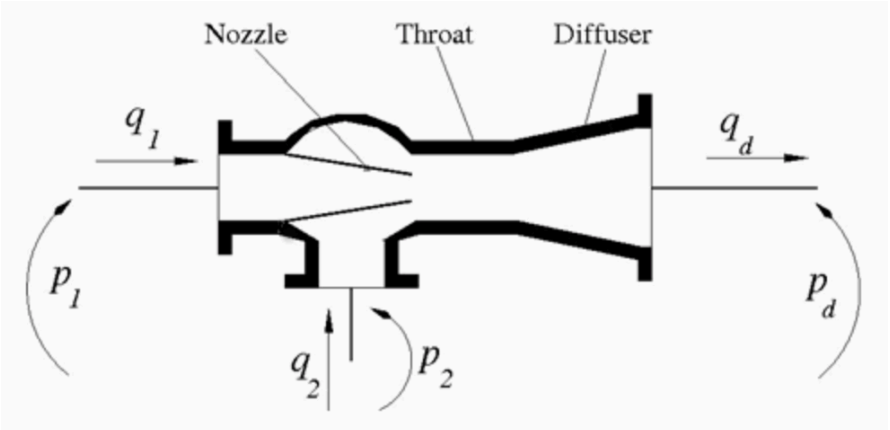

Figure 4.13: Sketch of the jet pump for the created model

In order to determine the equations useful to evaluate the possible discharge pressure, it was necessary to determine some parameters.
The first parameter is the diffuser area ratio calculated as:

$$a = \frac{A_{th}}{A_d}$$

Where:

- A_{th} is the throat area that is usually two to four times larger than the nozzle area;
- A_d is the diffuser outlet area, which corresponds to the ratio between the inlet and outlet diffuser areas. For a standard pump with a 5° – 7° included-angle diffuser, the ratio is close to 0.2;

With "b" the ratio between the nozzle area and the throat area is indicated:

$$b = \frac{A_n}{A_{th}}$$

Equation 4.5: Ratio between nozzle area and throat area

Where:

- An is the nozzle area;

For the case studied, the data shown in table 4.4 was used. The values relative to the loss coefficients in the different zones of the jet pump have been taken from the literature.

Characteristic value of the JP	Symbol	
Nozzle area m^2	A_n	0,0000785
Throat area m^2	A_{th}	0,001256
Diffuser inlet/outlet area ratio		0,224
Nozzle loss coefficient	K_n	0,05
Throat entry loss coefficient	K_{en}	0,05
Throat loss coefficient	K_{th}	0,1
Diffuser loss coefficient	K_{di}	0,1
Diffuser area ratio	a	0,2240
Nozzle/Throat area ratio	b	0,0625

Table 4.4: Characteristic parameters of the jet pump model

In order to apply the equation 4.6 it is necessary to determine the ratio between the primary flow rate pumped to the nozzle and the nozzle area, multiplying by the density:

$$Z = \rho \frac{q_1^2}{2A_n^2}$$

Where:

- q_1 is the primary flow rate pumped to the nozzle;
- A_n is the nozzle area, this parameter must be greater than 0;

The parameter "M" is the ratio between the primary flow rate pumped through the nozzle and the secondary flow rate:

$$M = \frac{q_2}{q_1}$$

Equation 4.6: Ratio between the primary flow rate and the secondary flow rate

Where:

- q_2 is the secondary flow rate;

Some of the previous parameters have therefore been used in the equation 4.7, through which it was subsequently possible to determine the discharge pressure.

$$p_d - p_0 = Zb^2(\frac{2}{b} + \frac{2}{1-b}M^2 - (1-M^2)(1 + k_{th} + k_{di} + a^2))$$

Equation 4.7: Difference between discharge pressure and throat pressure

Where

- k_{th} is the throat hydraulic loss coefficient, this parameter must be greater than 0;
- k_{di} is the diffuser hydraulic loss coefficient, this parameter must be grater than 0;

Applying Bernoulli's theorem inside the ejectors it has been possible to determine the throat pressure "P_0" with the equation:

$$P_0 = \left(P_1 + \frac{1}{2} v_1^2 \rho\right) + \left(P_2 + \frac{1}{2} v_2^2 \rho\right) - \Delta P - (\frac{1}{2} v_{th}^2 \rho)$$

Equation 4.8: Bernoulli's theorem to determine throat pressure

In the equation 4.8 the value of ΔP corresponds to the pressure losses in the nozzle area. After calculating the throat pressure it is easy to find the discharge pressure by reversing the equation 4.9 obtaining the following equation:

$$p_d = Zb^2 \left(\frac{2}{b} + \frac{2}{1-b} M^2 - (1 - M^2)(1 + k_{th} + k_{di} + a^2)\right) + p_0$$

Equation 4.9: Discharge pressure

For the case discussed above, having a primary flow rate of 8 m^3/h and a secondary flow rate of 15m^3/h the values of throat pressure and discharge pressure that have been found are listed in the table

Throat pressure	Discharge pressure
bar	bar
1,047	2,501

Table 4.5: Some result of the jet pump model

After having contacted several companies that manufacture this type of product and after having evaluated the technical data sheets and prices, it was decided to order the component from GEA, which made it tailored to our needs and the parameters calculated in the model.

4.6 Sensor

In order to measure the pressure and the flow rate, different types of sensors have been installed on the new configuration of the flushing rig under study.

4.6.1 Flow meter

On the flushing rig, considering the new configuration, two Nixon Turbin Flowmeter (of the type NT48-2" that has the range of 0(110) – 1100 LPM for water) are mounted. The accuracy of the meter is ± 0.5 %. The output is induced sinus pulses of 70-800 mV.

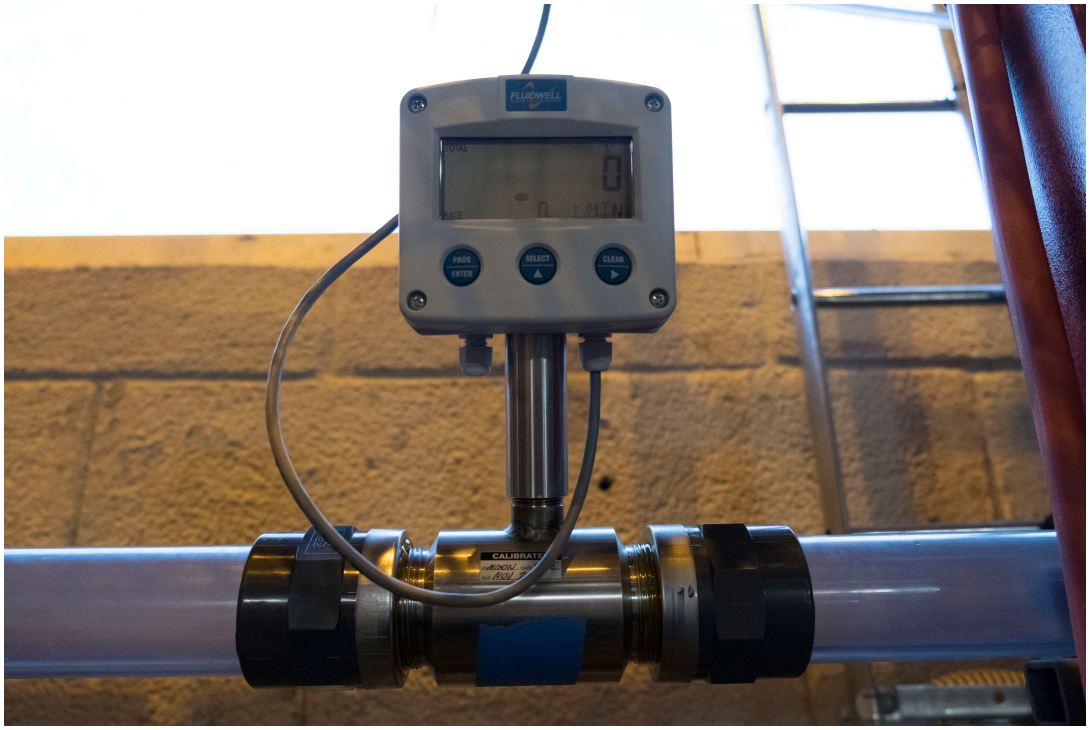

Figure 4.14: Flow meter installed on the flushing rig.

A F110P-AP-HD-OT-BP-ZC Fluidwell Process Indicator was already present in the IGP laboratory. This instrument acts as a transmitter and there is also a display for showing the flow rate and total flow. The k-factor of the indicator is separate for the total flow and the flow rate. An average k-factor from experimental tests was given by the producer as 46.53579 pulses/L, with linearity over a full range of 0.473608 %. The output for AP is 4-20 mA passive and for OT a pulse transistor.

4.6.2 Pressure sensor

In the new configuration, three pressure sensors have been positioned. The first pressure sensor is located in the upper left side of the U-shaped jumper, precisely at the height of the first elbow, instead the other two pressure sensors are positioned respectively before and after the jet pump. The type is from the UNIK 5000 pressure-sensing platform, more precisely the PTX 5072-tc-al-ca-h1-pa. This is a resistive pressure transducer where an output signal of 4-20 mA is proportional to the pressure applied. According to General Electric Company (2014) the sensors are a good solution for reliable, accurate and economical measurements in a long term. More detailed information about the pressure sensor located in the flushing rig can be found in the Appendix C.

4.7 Method to determine the volume fraction inside the pipes

In the previous work by Folde (2017), in order to calculate the volume fraction of the liquids present in the jumper, the system was drained into 15 L transparent buckets that has a measurement scale from 1 to 12 L, with steps of 0.1 L. The measurement readings uncertainty has been estimated in ± 0.1 L. The transparency made it simple to distinguish between red colour Exxsol D60 and tap water and, as a consequence, it was possible to determine the volume fraction.

Considering the new configuration, it would probably have been more complex to drain the liquid in a bucket and, consequently, this could have led to more uncertainty in the final result. It was therefore useful to find a new method to determine the volume fraction inside the pipes.

Starting from the assumption that both the total volume of the jumper and the diameter are known (as a consequence also the radius), a ruler has been glued on each horizontal tube of the jumper in order to determine the level of the oil-water interface as it is possible to observe in figure 4.15.

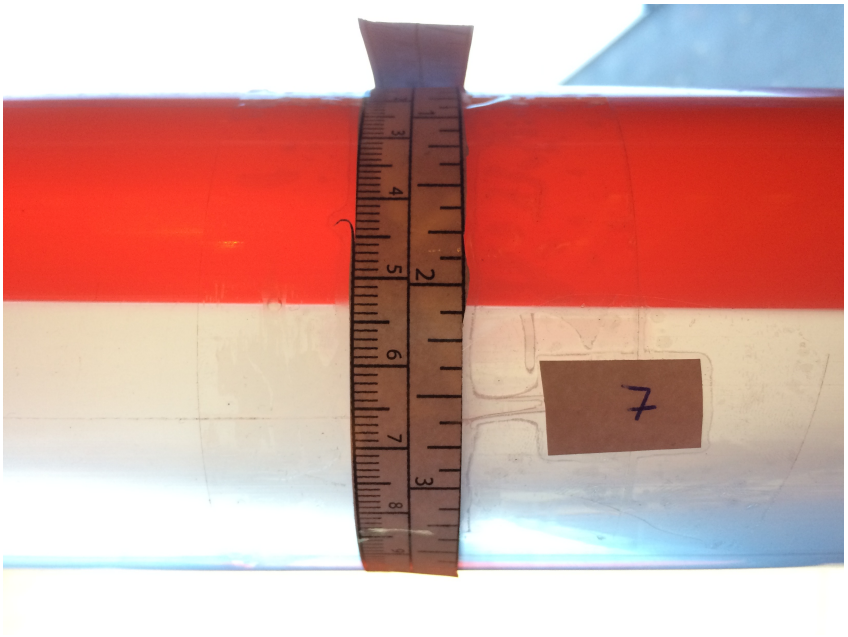

Figure 4.15: Meter placed on the pipe for the determination of the volume fraction.

During the experiments, several photos were taken at different time steps at all the meters located in different parts of the jumper so as to be able to determine subsequently the parameter "S" which is, as it is possible to see in figure 4.16, simply the measure of the oil height with respect to the height of water, read on the meter placed on the pipes.

After determining the parameter “S”, already knowing the dimension of the radius "r", it is easy to

go back to the parameter "θ" which is the angle:

$$\theta = \frac{S}{r}$$

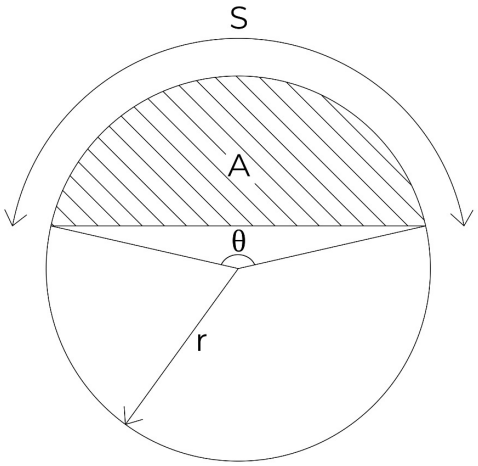

Figure 4.16: Sketch of the method for determining the oil volume fraction

Determined this angle, with the equation 4.10 the area occupied by the oil was calculated.

$$A = \frac{r^2}{2}(\theta - sin\theta)$$

Equation 4.10: Area occupied by the oil

Knowing the area occupied by the oil and the length of the pipe it is easy to determine the diameter with the equation 4.11.

$$V = A \cdot h$$

Equation 4.11: Volume occupied by the oil

In order to have a more precise volume fraction value, two rulers were placed on each pipe, one at the beginning and one at the end of the pipe, respectively. The value of volume fraction is therefore determined by averaging between the measurements on the two meters of the same pipe.

As is well known, the U-shaped jumper is composed of both horizontal and vertical pipes. However, the previous method cannot be used to determine the volume fraction for the vertical part of the flushing rig as the two fluids have distinctly different densities and so they separate quickly as shown in the figure 4.17. Reading the height of the oil in relation to the water using the previous method would therefore not have given accurate results.

Figure 4.17: Oil column in the vertical part of the jumper.

Since the oil has a difference density with respect to water, the two phases eventually separate t and it is therefore easy, knowing the characteristics dimensions of the pipes, to calculate the height of the oil column in relation to the overall length of the pipe. Knowing the height of the pipe occupied by the oil and the height of the pipe occupied by the water, it is therefore possible to calculate the volume and consequently the volume fraction for the two fluids.

The total volume of the jumper is known, so adding the data collected from the analysis of all the pipes, the total volume fraction was determined.

5. Numerical simulation with LedaFlow

Within this thesis work various simulations of what was then carried out in the laboratory were performed. The simulations were performed with the LedaFlow simulator, taking into consideration the different properties of the fluids, the characteristics of the tubes, the characteristic parameters of the pumps and the environmental conditions present in the laboratory.
The simulations are executed to study different displacement rates, displacement times and displacement fluids.

5.1 General characteristics of the simulations in LedaFlow

LedaFlow simulator allows realizing different system configurations, inserting also components like pumps, valves, separator, and considering factors like leaks in pipes. For the case studied, two different models were considered. The first model consist of only the U-shaped jumper, an inlet and outlet node, instead the second model takes into account the presence of different pipes for the recirculation of the fluids, a pump and a source.
These systems are used both to study the water that displaces oil and to study the oil that displaces water. The tube is initially filled with the fluid to be displaced.
The fluids that are used for both simulations are tap water and oil Exxsol D60. This particularly type of oil is produced from petroleum-based raw materials which are treated with hydrogen in the presence of a catalyst to produce a low smell, low aromatic hydrocarbon solvent. The major components include normal paraffin, isoparaffins, and cycloparaffins.

The main characteristics of the fluids that have been inserted to set the models are listed in the table below.

	Density	Viscosity	Compressibility	Conductivity	Heat Capacity	Molar mass
	kg/m^3	Pa s	Kg/m^3/bar	W/m-K	J/kg-K	g/mol
Water	998,9	0,001095	0,0391	0,6069	4183,8	18,02
Oil (Exxsol D60)	786	0,00156	0,0391	0,136	1760	158

Table 5.1: Principal characteristics of the fluid used for the simulations

LedaFlow also allows entering the parameters that characterize the material of which the U-jumper and the others pipes are made, in this case PVC. The properties useful to set the models created in LedaFlow are presented in the table 5.2.

Property	Symbol	Value
Density	ρ_{PVC}	1400 Kg/m^3
Heat capacity	c_p	1005 J/ Kg °C
Conductivity	k	0,19 W/(m K)
Emissivity	ε	0,92
Young's modulus	E	3,25 Gpa
Viscosity	μ_{PVC}	0 Pa-s
Thermal expansion coefficient	α	0 1/C

Table 5.2: Characteristics parameter of the PVC pipes

5.2 Geometry and characteristics of the first model

As described previously, the first model is built taking into account only the U-shaped jumper, an inlet and outlet nodes. For the nodes placed at the beginning and at the end of the jumper, temperature and pressure conditions were chosen over time. In the inlet node it is also possible to set the flow rate, expressed in kg/s.

Figure 5.1: Network of the U-shaped jumper in LedaFlow

In the pipe settings are the profile and geometry of the pipe, as well as the mesh constructed. The profile is created in a Cartesian coordinate system, in two dimensional, using *X* and *Z*. The measures are initially based on the thesis of Opstvedt (2016) with some adjustments made by Folde (2017) to fit the measured drainable volume of 165.98 L.

However, according to the experiment conducted by Folde (2017), it should be noticed that after all of the experiments conducted, the average measured total volume was 165.0 L ± 0.3 L.

In order to make a more accurate model, the variation in diameter in the elbows has been taken into account, as it is possible to observe from the table 5.4. The characteristic dimensions of the jumper are shown in the table 5.3.

X	Y	Z	L
[m]	[m]	[m]	[m]
0	0	1,81	0
1,536	0	1,81	1,536
1,696	0	1,71	1,725
1,696	0	0,16	3,275
1,856	0	0	3,501
4,856	0	0	6,501
5,016	0	0,16	6,727
5,016	0	2,16	8,727
5,14	0	2,24	8,875

Table.5.3: Profile of the U-jumper in LedaFlow

In table 5.4 it is possible to observe the geometry of the model. It is providing the internal diameter, which is varying based whether it is a bend (160mm) or regular transparent PVC pipe (153,6mm), for the calculated length of the profile L. The absolute roughness for a PVC pipe is given as ε = 0,0015 mm (SulzerPumpesLtd). In addition, the thickness of the pipe is specified as t = 3,2 mm.

Length of pipe profile	Internal diameter
[m]	[mm]
0	153,6
1,536	160,0
1,725	153,6
3,275	160,0
3,501	153,6
6.501	160,0
6,727	153,6
8,727	160,0
8,875	160,0

Table.5.4: Geometry and diameter of U-jumper in LedaFlow

From the values expressed in the previous tables, the constructed jumper model is shown in the figure 5.2.

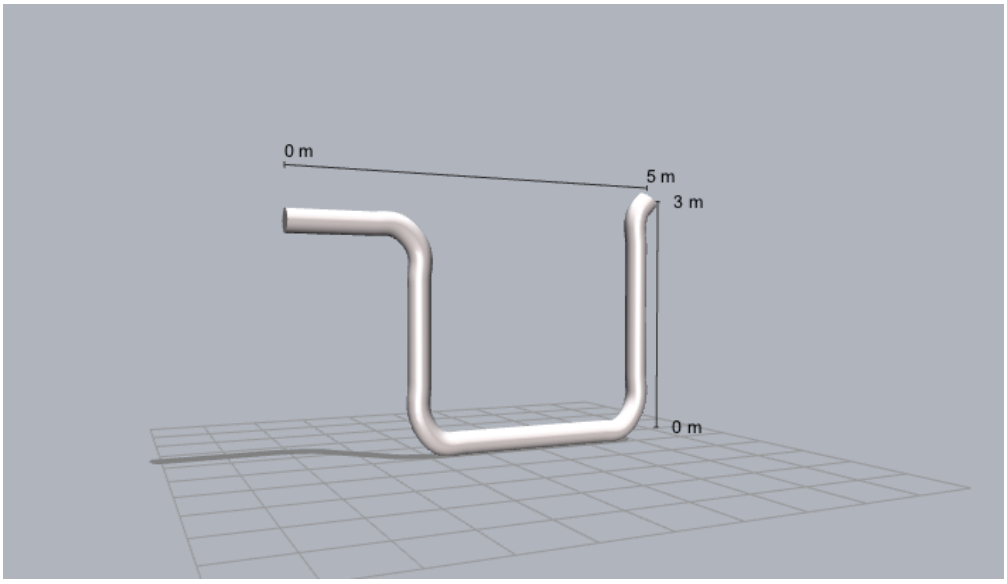

Figure 5.2: U-jumper constructed by Leda Flow simulator.

5.3 Geometry and characteristics of the new model

In order to obtain a more reliable result from the simulations carried out with LedaFlow, a more complete model has been created, able to simulate the recirculation line that characterizes the new layout of the flushing rig.

This new method takes into account, in addition to the U-shaped jumper, also some pipes for the recirculation of the fluids, a source (indicated with a green arrow) a centrifugal pump, a valve and a separator. Among the instruments available in LedaFlow it is impossible to insert a jet pump, so in order to simulate its operation we decided to insert a centrifugal pump and source in order to recirculate the fluid.

The characteristic dimensions of the U-shaped jumper are the same indicated in the previous chapter for the first model.

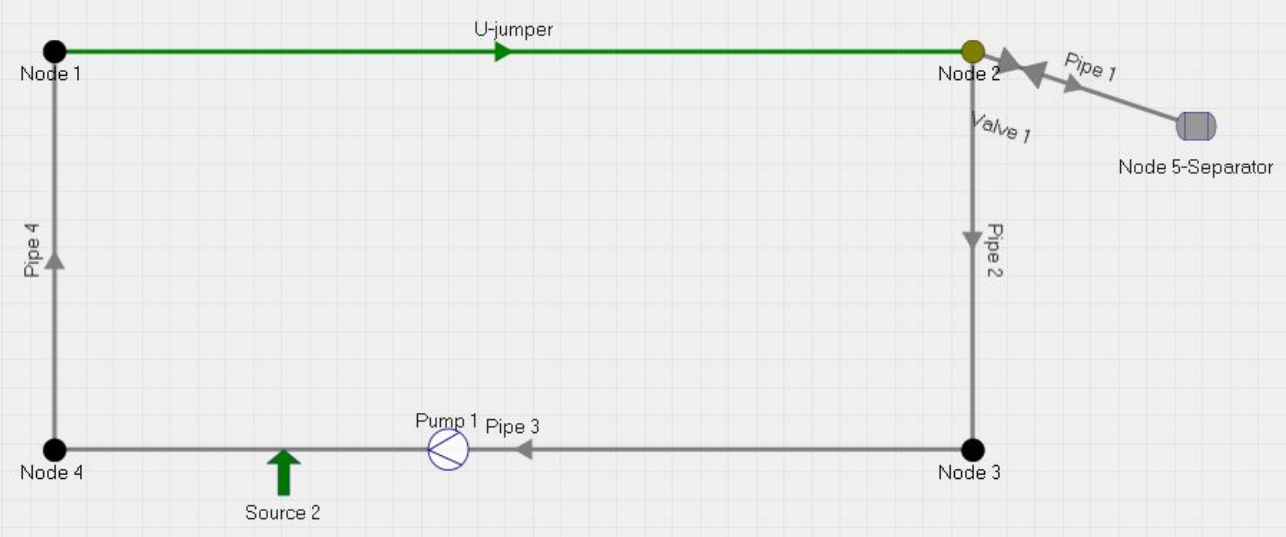

Figure 5.3: Network of the complete configuration builded in LedaFlow

As it is possible to observe from the figure 5.3 the new configuration is composed of, in addition to the jumper, others 4 pipes. Also for this type of configuration, PVC pipes were considered, with the same material characteristics of the pipes used for the first model. The absolute roughness for a PVC pipe is given as $\varepsilon = 0.0015$ mm (SulzerPumpesLtd).

The lengths of the recirculation pipes, listed in the table below, are not exactly the same of the structure build in the laboratory, but are very similar and therefore able to provide a good approximation.

Pipe 1			
X	Y	Z	L
[m]	[m]	[m]	[m]
5,14	0	2,24	0
3	0	2	2,15

Pipe 2			
X	Y	Z	L
[m]	[m]	[m]	[m]
5,14	0	2,24	0
5,14	0	0	2,24

Pipe3			
X	Y	Z	L
[m]	[m]	[m]	[m]
5,14	0	0	0
0	0	0	5,14

Pipe 4			
X	Y	Z	L
[m]	[m]	[m]	[m]
0	0	0	0
0	0	1,81	1,81

Table.5.5: Profile of the pipes that make the recirculation line in LedaFlow

The characteristics internal diameters and the length for the recirculation pipes are inserted in the tables below. In this case the diameters perfectly match the dimensions of those present in the new configuration of the flushing rig builded in the laboratory, in fact the pipes diameter before the jet pump are characterized by a smaller diameter than that of the pipes placed after the pump.

Pipe 1	
Length of pipe profile	Internal diameter
[m]	[mm]
0	57
2,15	57

Pipe 2	
Length of pipe profile	Internal diameter
[m]	[mm]
0	63
2,24	63

Pipe3	
Length of pipe profile	Internal diameter
[m]	[mm]
0	63
5,14	63

Pipe 4	
Length of pipe profile	Internal diameter
[m]	[mm]
0	75
1,81	75

Table.5.6: Geometry and diameter of the pipes that make the recirculation line in LedaFlow

5.4 LabView

LabVIEW (Laboratory Virtual Instrumentation Engineering Workbench) is the integrated development environment for the National Instruments visual programming language. With the aim of recording the measured values from all the three pressure sensors and the two flow meters described in the previous chapter, the LabView software was used. The block diagram for the studied case is visualized in Figure 5.4.

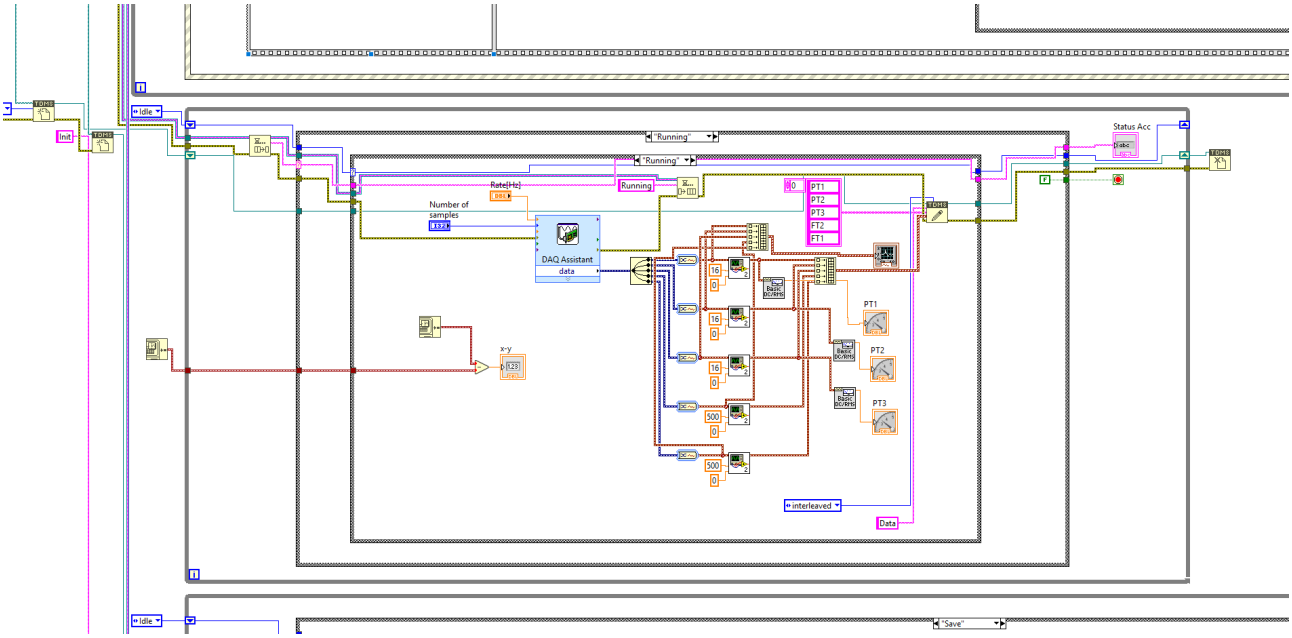

Figure 5.4: Virtual instrumentation block diagram with LabView

6. Results

In this chapter the results obtained through the mathematical model and the simulations that have been realized with LedaFlow are presented. Additionally, a comparison between all the results of the experiments carried out in the laboratory is given; unfortunately, there is not a huge amount of values due to time constraints that did not allowed to reproduce many experiments in the laboratory. It was therefore decided to reproduce only the cases in which water displace oil with three different injected flow rates.

6.1 LedaFlow simulation with simple configuration

Considering the model created with LedaFlow is made up only of the jumper, simulations were performed both for the case in which water displacing oil and for oil displacing water, starting from different injected flow rate. The results are shown in this chapter.

6.1.1 Oil displacing water

The results from the LedaFlow simulation where oil is displacing water are displayed in Table 6.1. As you can see from the table below, four different simulations have been conducted, characterized by a different injected flow rate. The boundary conditions (geometry of the jumper and characteristic parameters of the fluids are the same) remain unchanged.

	5 m^3/h	8 m^3/h	12 m^3/h	20,77 m^3/h
Time	Water VF LedaFlow	Water VF LedaFlow	Water VF LedaFlow	Water VF LedaFlow
[s]	[-]	[-]	[-]	[-]
0	1	1	1	1
20	0,8036	0,6925	0,5365	0,2312
40	0,6135	0,3905	0,2279	0,0550
60	0,4322	0,2733	0,1574	0,0324
80	0,3648	0,2380	0,1360	0,0272
80	0,3648	0,2380	0,1360	0,0272
100	0,3448	0,2280	0,1340	0,0272
120	0,3391	0,2170	0,1302	0,0255
140	0,3371	0,2133	0,1302	0,0254
180	0,3363	0,2101	0,1300	0,0253
220	0,3360	0,2061	0,1300	0,0252
260	0,3358	0,2069	0,1300	0,0252
300	0,3357	0,2068	0,1300	0,0252
400	0,3355	0,2060	0,1300	0,0252

500	0,3355	0,2060	0,1300	0,0252
600	0,3354	0,2050	0,1300	0,0252
700	0,3354	0,2050	0,1300	0,0252

Table 6.1: Results for the case in which oil displacing water

In addition the previous results are plotted in figure 6.1. As a general rule for all the four cases studied, we can state that during the first 60 seconds there is a very rapid removal of the fluid (in this case water). After the first 60 seconds, the percentage of removed fluid remains almost constant.

Observing the data shown in the table and the graph in the figure below, it can be seen that as the injected flow rate increases, the time to displace the fluid (in this case water) decreases. As a matter of fact, by performing the simulation with low flow rates, we can observe that a high percentage of non-removed fluid will remain.

Analysing the case of an injected flow rate equal to 5 m^3/h, it is observed that there will always be a remaining water volume fraction between 30% and 40%. By significantly increasing the flow rate up to 8 m^3/h a better performance is achieved, in fact the water volume fraction that can be reached is between 18% and 22% after 700 seconds.

Finally, by imposing a flow rate of 20.77 m^3/h, a water volume fraction of less than 10% is achieved within the first 40 seconds.

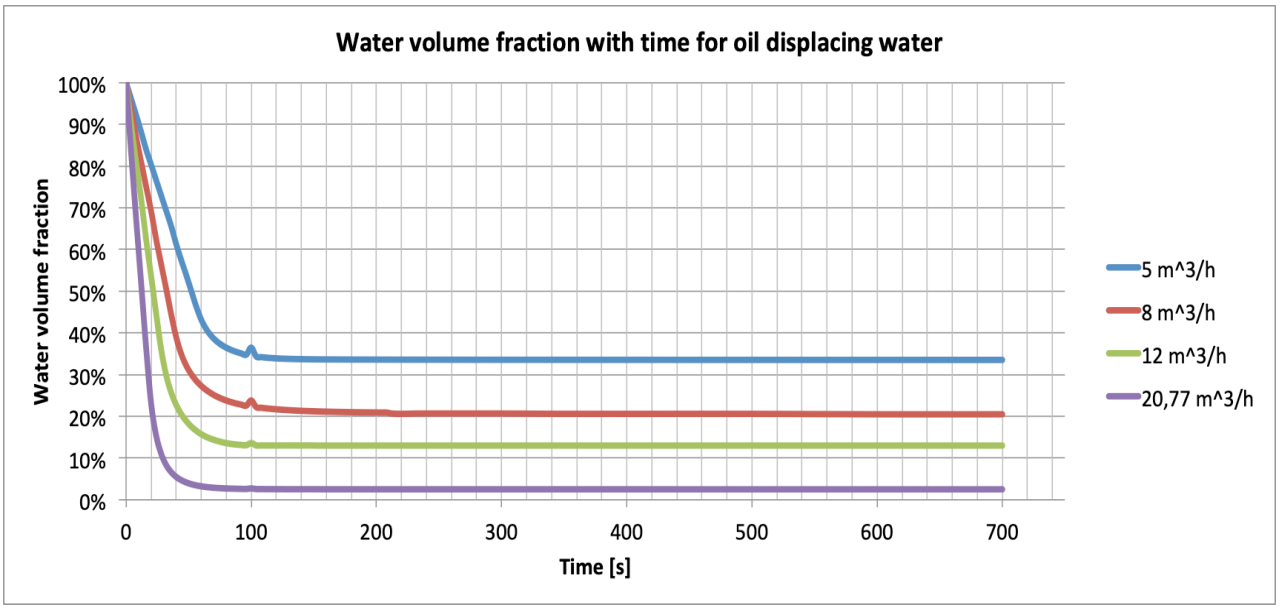

Figure 6.1: LedaFlow results for oil displacing water in simple configuration

6.1.2 Water displacing oil

The results from water displacing oil are presented in Figure 6.2 and Table 6.2. The graph and the table are presenting the oil volume fractions as a function of time for four different flow rates which are the same simulated for the previous case in which oil displacing water.

	5 m^3/h	8m^3/h	12 m^3/h	20,769 m^3/h
Time	Oil VF LedaFlow	Oil VF LedaFlow	Oil VF LedaFlow	Oil VF LedaFlow
[s]	[-]	[-]	[-]	[-]
0	1	1	1	1
20	0,8531	0,7629	0,6400	0,3998
40	0,7098	0,5251	0,2878	0,1449
60	0,5602	0,2891	0,1894	0,0946
80	0,4122	0,2170	0,1518	0,0731
100	0,2791	0,2058	0,1398	0,0662
120	0,2735	0,2014	0,1345	0,0629
140	0,2710	0,1989	0,1314	0,0605
180	0,2682	0,1962	0,1279	0,0599
220	0,2668	0,1944	0,1251	0,0599
260	0,2657	0,1928	0,1233	0,0599
300	0,2639	0,1914	0,1230	0,0599
400	0,2619	0,1903	0,1230	0,0599
500	0,2607	0,1902	0,1230	0,0599
600	0,2603	0,1902	0,1230	0,0599
700	0,2602	0,1902	0,1230	0,0599

Table 6.2: Results for the case in which water displacing oil

Observing the chart also in this case we can state that, as a general rule, for all the four cases it can be seen that during the first 100 seconds we have a very rapid removal of the fluid (in this case oil). After the first 100 seconds the percentage of removed fluid remains almost constant.

Indeed, it is possible to state that increasing the injected flow rate, the time to displace the fluid (in this case oil) decreases.

It should be noticed that it seems like the displacement ability for a water flow rate to displace the oil in the system is higher than the one for an oil rate displacing water in the system. This might be due to differences in flow rate, density or viscosities.

From the processed data and the chart in figure 6.1 and 6.2 it is possible to see that, with this type of configuration, imposing lower flow rates the efficiency is higher in the case of water that displacing oil. It is possible to observe that, imposing a flow rate of 5 m^3/h at 700 seconds we will have a water

oil volume fraction less than 30%. In the case in which water displacing oil, imposing the same flow rate at 700 seconds, it is observed a water volume fraction between 32% and 35%.

On the contrary, instead, as can be seen from the data collected in the tables 6.1 and 6.2, if the maximum flow rate of 20.77 m^3/h is imposed, the efficiency is higher in case in which oil displacing water.

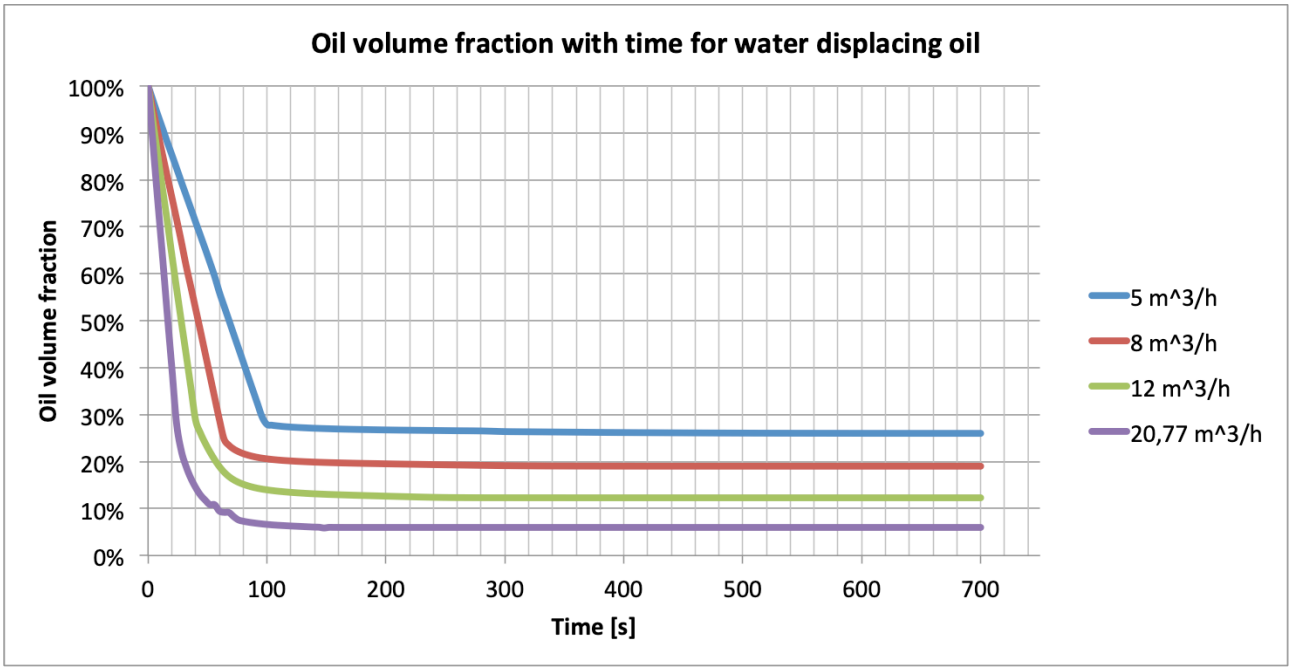

Figure 6.2: LedaFlow results for water displacing oil in simple configuration

6.2 LedaFlow simulation with complete configuration

In this chapter all the results of the simulations realized with the second configuration, that is the one composed of the centrifugal pump and the source (which simulate the action of a jet pump) and the recirculation line, are collected.
Also for this case study are simulated both the case in which water displacing oil and the case in which oil displacing water. The data expressed in the following chapters refer only to the U-shaped jumper, do not take into consideration the measurements made in the other parts of the recirculation line, this also to facilitate the comparison between the different models.

6.2.1 Oil displacing water

The results of the LedaFlow simulation of oil displacing water are given in table 6.3, and plotted in Figure 6.3. Both the features are presenting the water volume fractions as functions of time for five different injected flow rates flow rates.

The results collected with this type of simulation are about seventy, but for simplicity of reading in Table 6.3 there have been inserted only sixteen of them.

By analysing the values expressed in the table for this type of simulation it is possible to state that increasing the injected flow rate decreases the time to displace the fluid. It can be observed, for example, that by injecting an oil flow rate equal to 8 m^3/h a value of less than 10% of water is reached after about 220 seconds, instead injecting an oil flow rate equal to 12 m^3/h is found less than 10% of water after only 120 seconds.

	5 m^3/h	8 m^3/h	10 m^3/h	12 m^3/h	20,77 m^3/h
Time	Water VF LedaFlow	Water VF LedaFlow	Water VF LedaFlow	Water VF LedaFlow	Water VF LedaFlow
[s]	[-]	[-]	[-]	[-]	[-]
0	1	1	1	1	1
20	0,8349	0,7468	0,6895	0,6344	0,4135
40	0,6940	0,5478	0,4663	0,3971	0,2004
60	0,5656	0,3978	0,3184	0,2603	0,1197
80	0,4554	0,2926	0,2296	0,1878	0,0813
100	0,3662	0,2251	0,1784	0,1446	0,0614
120	0,2972	0,1828	0,1450	0,1163	0,0484
140	0,2449	0,1541	0,1213	0,0964	0,0397
180	0,1772	0,1163	0,0901	0,0702	0,0302
220	0,1392	0,0924	0,0703	0,0543	0,0258
260	0,1154	0,0757	0,0570	0,0441	0,0240

300	0,0987	0,0636	0,0477	0,0372	0,0233
400	0,0713	0,0448	0,0341	0,0280	0,0227
500	0,0550	0,0349	0,0279	0,0246	0,0225
600	0,0452	0,0296	0,0251	0,0234	0,0225
700	0,0388	0,0266	0,0238	0,0229	0,0225

Table 6.3: Results for the case in which oil displacing water in complex configuration

As can be seen in the chart in figure 6.3, even with this type of simulation, there is a rapid decrease in the fluid that is displaced in the first one hundred seconds. At the end of the entire period of 700 seconds, despite the injecting flow rates that are clearly different from one another, the remaining volume fraction is very similar.

From the results expressed in table 6.3 it is possible to notice that by injecting initial oil flow rate of $12m^3/h$ or initial oil flow rate of $20.77m^3/h$ the final water volume fraction difference at 700 seconds is about 0.005%.

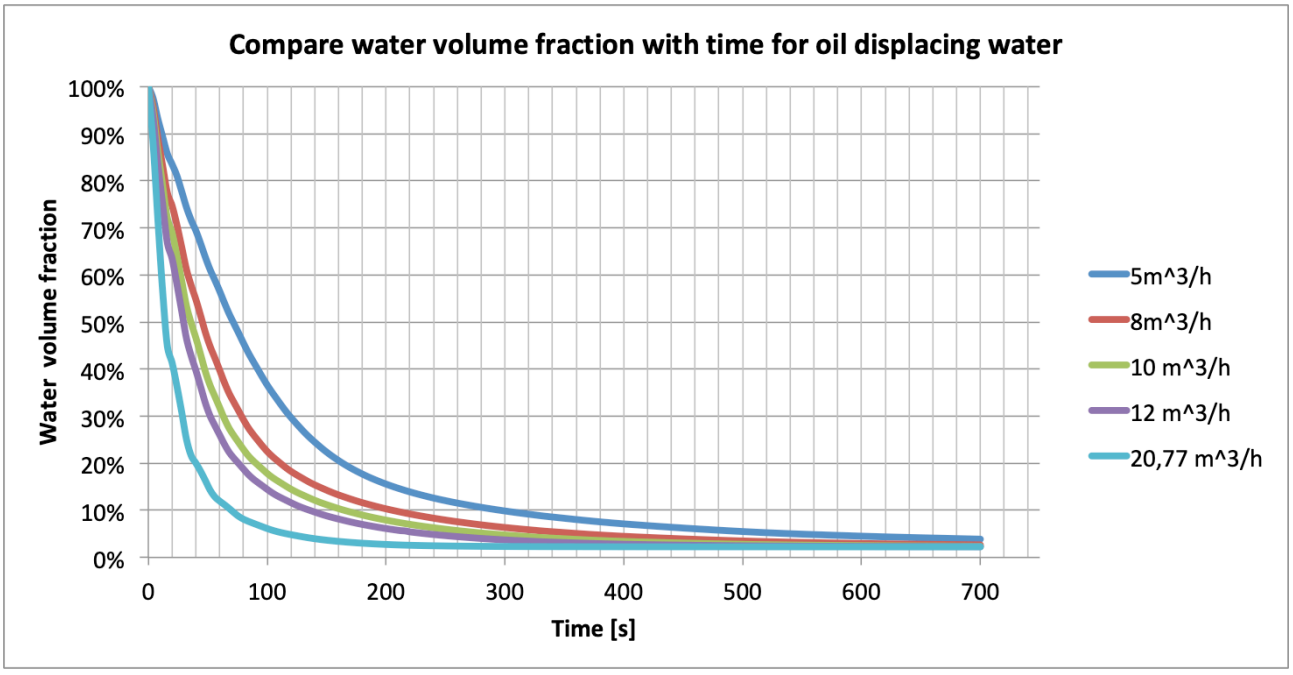

Figure 6.3: LedaFlow results for oil displacing water in complex configuration

6.2.2 Water displacing oil

Figure 6.4 shows the oil volume fraction with time during the LedaFlow simulation for water displacing oil, and in table 6.4 the numerical results are presented. Following the same procedure of aforementioned cases, we proceeded by imposing different injected flow rates during the simulation and evaluating the volume fraction over time within the U-shaped jumper.

	5 m^3/h	6,5 m^3/h	8 m^3/h	10 m^3/h	12 m^3/h	20,77 m^3/h
Time	Oil VF LedaFlow	Oil VF LedaFlow	Oil VF LedaFlow	Oil VF LedaFlow	Oil VF LedaFlow	Oil VF LedaFlow
[s]	[-]	[-]	[-]	[-]	[-]	[-]
0	1	1	1	1	1	1
20	0,8833	0,8516	0,8195	0,7774	0,7357	0,5299
40	0,7810	0,7244	0,6707	0,6046	0,5447	0,3182
60	0,7020	0,6318	0,5670	0,4901	0,4247	0,2169
80	0,6424	0,5627	0,4901	0,4087	0,3425	0,1603
100	0,5946	0,5073	0,4305	0,3478	0,2835	0,1227
120	0,5534	0,4609	0,3823	0,3006	0,2395	0,0972
140	0,5177	0,4215	0,3425	0,2631	0,2056	0,0798
180	0,4589	0,3586	0,2813	0,2077	0,1575	0,0580
220	0,4124	0,3110	0,2366	0,1691	0,1255	0,0452
260	0,3749	0,2738	0,2026	0,1409	0,1033	0,0340
300	0,3440	0,2439	0,1758	0,1198	0,0872	0,0288
320	0,3305	0,2310	0,1645	0,1111	0,0808	0,0267
340	0,3180	0,2192	0,1543	0,1035	0,0752	0,0247
400	0,2860	0,1891	0,1291	0,0853	0,0624	0,0222
500	0,2451	0,1516	0,0996	0,0656	0,0495	0,0218
600	0,2141	0,1244	0,0800	0,0537	0,0378	0,0218
700	0,1893	0,1040	0,0665	0,0448	0,0293	0,0218

Table 6.4: Results for the case in which water displacing oil in complex configuration

As with respect to the previous cases, it is easy to state that increasing the injected flow rate reduces the time to remove fluid.

On the other hand, when water displaces oil, differently from the previous case, we can observe from the chart in the figure 6.4 that injecting different flow rates, the volume fraction values given to the final time of 700 seconds are clearly different from each other. It might be than one has to flush for longer time for them to achieve a low oil content.

Analysing the first 15 seconds, the volume fraction is decreasing fast and close to linearly. This is most likely due to a piston displacement effect. The greater the injected flow rate is and the greater

effect this volume will have on the oil volume fraction, in fact it is possible to observe that injecting a flow rate of 20.77 m^3/h this effect lasts up to an oil volume fraction of about 54%, instead injecting a flow of 10 m^3/h or 12 $m^{\wedge 3}$/h the piston effect the oil volume fraction remain between 70% and 80%.

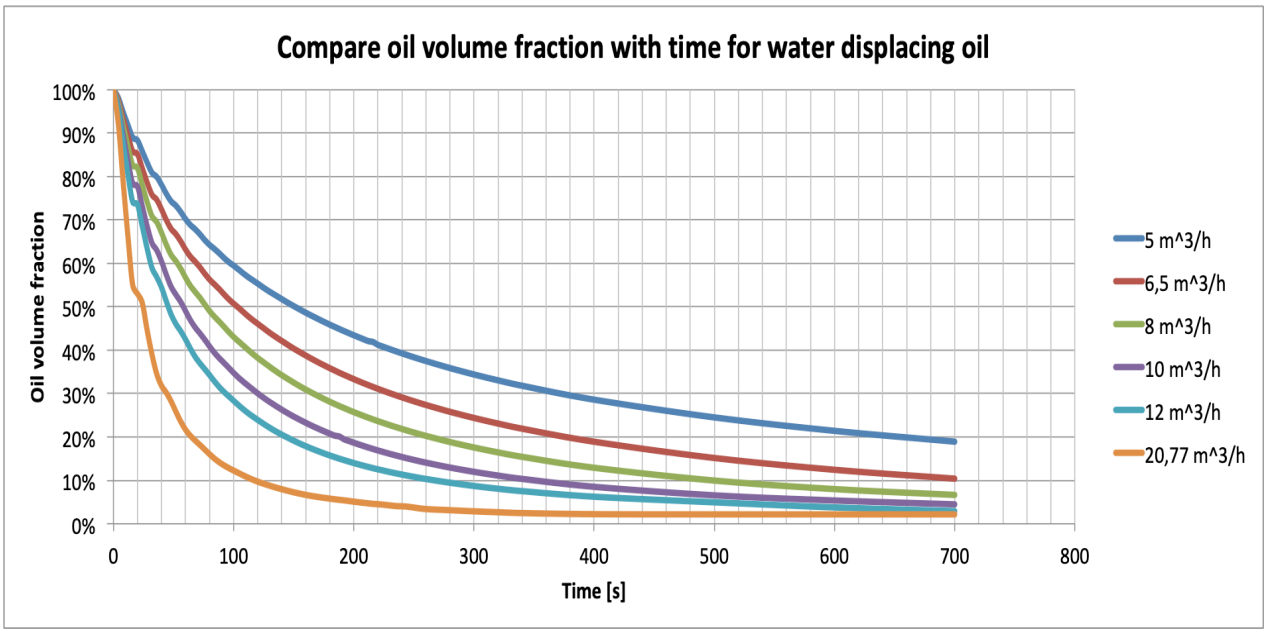

Figure 6.4: LedaFlow results for water displacing oil in complex configuration

6.2.3 Analysis of flow rate for water displacing oil

In the simulation made with LedaFlow, a constant pump pressure boost of 0.1 was imposed, and five different flow rates were injected in order to evaluate the flow rate (expressed in kg/s) inside the U-shaped jumper. Partial data obtained from the simulation are presented in the table below.

	5 m^3/h	8 m^3/h	10 m^3/h	12 m^3/h	20,77 m^3/h
Time	Flow rate	Flow rate	Flow rate	Flow rate	Flow rate
[s]	kg/s	kg/s	kg/s	kg/s	kg/s
0	0	0	0	0	0
20	8,634	8,487	8,424	8,374	8,292
40	8,673	8,650	8,584	8,579	8,854
60	8,846	8,871	8,877	8,925	9,269
80	8,933	9,015	9,107	9,189	9,484
100	9,015	9,170	9,297	9,392	9,628
120	9,104	9,316	9,456	9,552	9,727
140	9,183	9,446	9,589	9,680	9,787
180	9,311	9,661	9,795	9,864	9,847
220	9,448	9,826	9,943	9,984	9,881
260	9,623	10,010	10,092	10,095	9,856
300	9,673	10,058	10,128	10,120	9,854
400	9,882	10,235	10,247	10,192	9,758
500	10,036	10,340	10,304	10,199	9,959
600	10,156	10,402	10,327	10,147	9,960
700	10,252	10,438	10,260	10,144	9,961

Table 6.5: Value of the flow rate in the U-shaped jumper for water displacing oil

Analysing the results obtained, it can be observed that, by imposing a constant pressure boost for different injected flow rates, there is not a large variation in the flow rate through the jumper. From figure 6.5 it is possible to see that, after a rapid growth in the first 10 seconds, and several oscillations in the first 50 seconds (they are seen more clearly in the figure 6.6), the flow inside the jumper becomes almost constant.

Moreover, it can be seen that at the end of the simulation, at 700 seconds, injecting the highest flow rate, the flow rate inside the jumper is the lowest obtained.

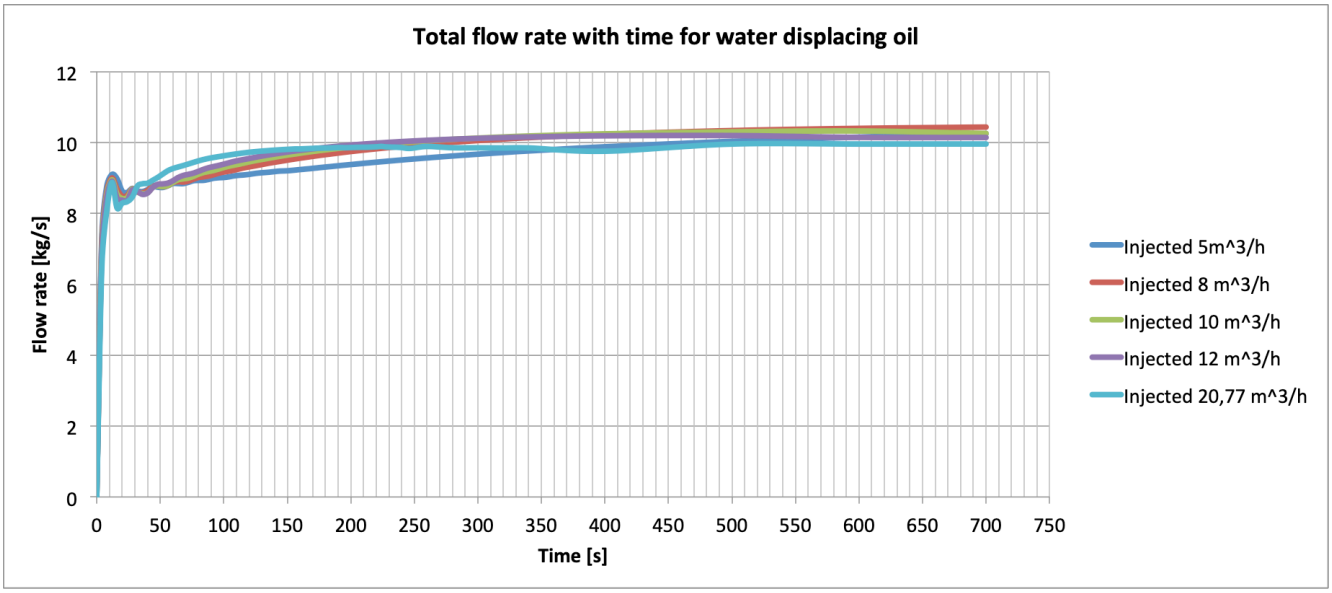

Figure 6.5: Flow rate for water displace oil imposing the same pressure boost of the pump

The chart in the figure 6.6 instead shows more specifically the first seconds of the simulation; as shown in the graph, it is evident that at the initial stage, injecting a greater flow rate, inside the jumper there is a lower flow compared to the other cases. For example, by initially injecting a flow rate of 20.77 m^3/h in the first few seconds inside the jumper the flow is lower than in the case in which a flow rate equal to 12 m^3/h is injected. After this phase, the flow rate in the jumper obtained by injecting 20.77m^3/h grows up to exceed all the others, and then decreases again until reaching the lowest range among those compared at the end of the simulation.

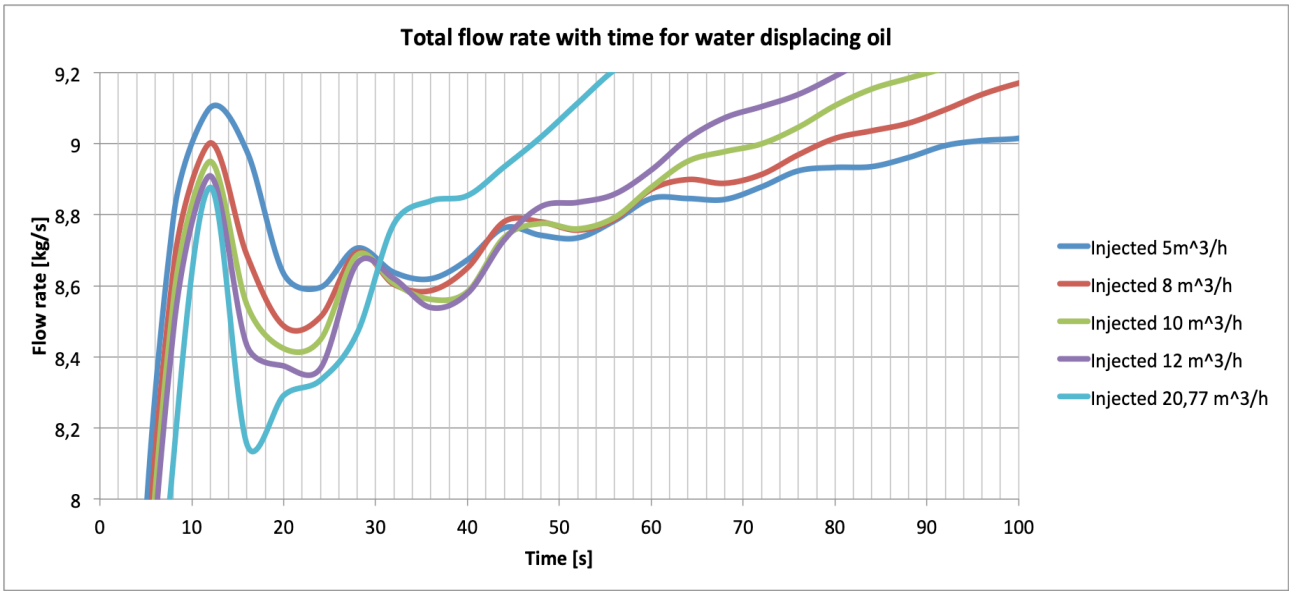

Figure 6.6: Zoomed view of the first few seconds of the flow rate for water displacing oil

6.2.4 Analysis of the effect of the imposed pressure boost for water displacing oil

It can be interesting to observe the behaviour of the oil volume fraction (always for the case in which water displacing oil) imposing a constant injected flow rate but varying the pressure boost of the centrifugal pump inserted in the model in LedaFlow.

In the case studied below, a constant flow rate of 12 m^3/h was set and the pump pressure boost was varied, taking into consideration values between 0.1 and 0.7 bar. During the simulations it was also tried to further reduce the pressure boost below the minimum value of 0.1 bar, but by injecting the fluid from the source, the latter ran the pipes in reverse direction because the pump was not able to convey it in the right direction. The minimum value of 0.1 bar was chosen precisely because it is the lowest value useful to make the fluid flow correctly in the flushing rig.

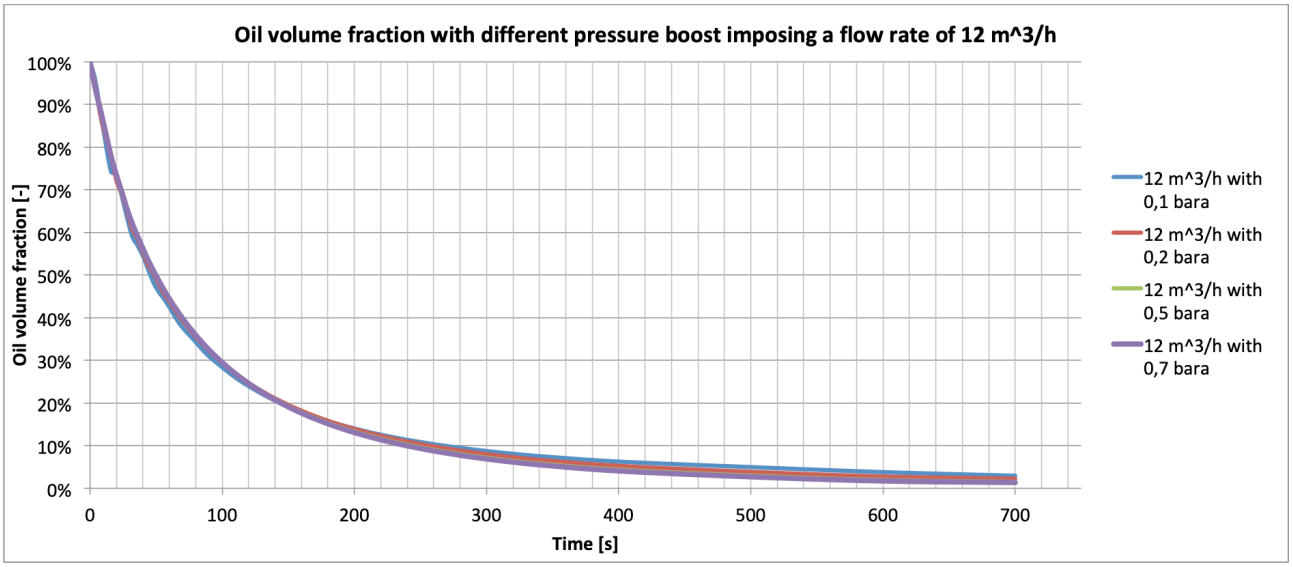

Figure 6.7: Oil volume fraction with time changing the pressure boost

As can be seen from the chart in figure 6.7 and from figure 6.8, which represent a detailed view of the first graph, the trend of the oil volume fraction imposing different values of pressure boost is very similar in all four simulated cases.

Watching closely at the chart in figure 6.8 we can state that, at the end of the time taken for the simulation (always 700 seconds), a higher-pressure boost will give better results in terms of oil volume fraction value in the jumper. In fact it is possible to observe that with a pressure boost of 0.7 there is a lower value of oil volume fraction.

By changing the pressure boost and leaving the injected flow rate constant, there are no major advantages in terms of oil removed from the water, at least for the case in which water displacing oil.

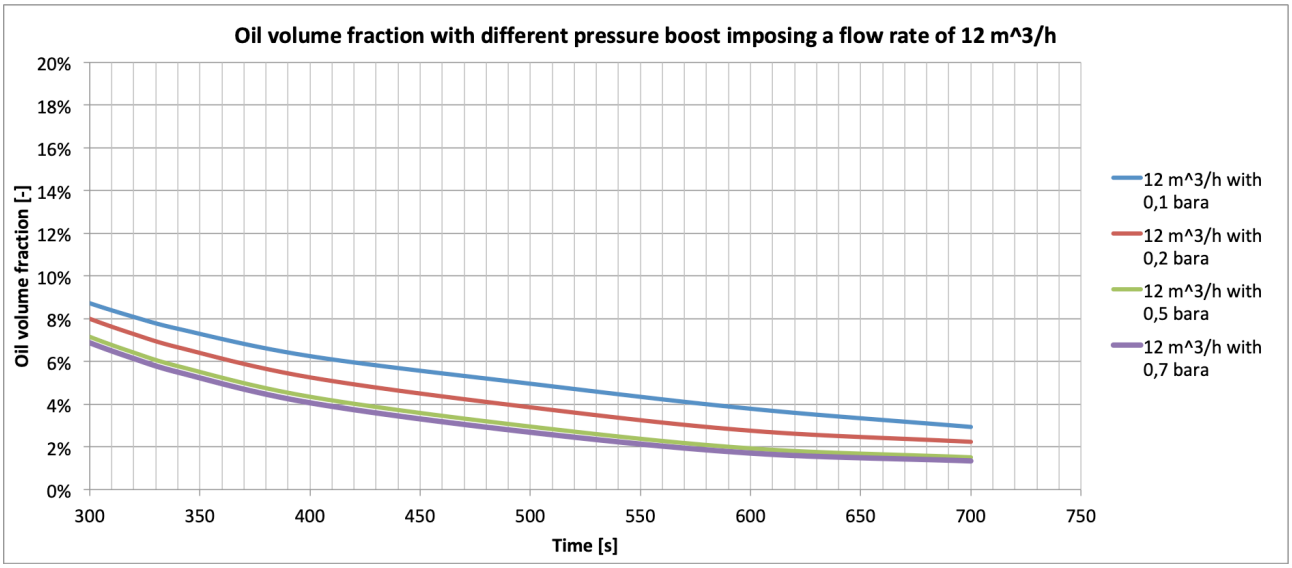

Figure 6.8: Details view for the chart in figure 6.7

Keeping the initial assumptions unchanged, a flow rate analysis within the jumper was also conducted. It is possible to conclude that by keeping the injection flow rate constant and increasing the pump pressure boost the flow rate inside the jumper also increases.

	12 m^3/h with 0,1bara	12 m^3/h with 0,2bara	12 m^3/h with 0,5bara	12 m^3/h with 0,7bara
Time	Flow rate	Flow rate	Flow rate	Flow rate
[s]	kg/s	kg/s	kg/s	kg/s
0	0	0	0	0
20	8,3745	13,1859	22,5805	27,5049
40	8,5786	13,6265	23,5914	28,7243
60	8,9255	13,9550	24,1660	29,4410
80	9,1892	14,2456	24,6043	29,9820
100	9,3923	14,4593	24,9669	30,4294
120	9,5522	14,6417	25,2625	30,7948
140	9,6799	14,7875	25,5048	31,0957
180	9,8636	15,0067	25,8683	31,5469
220	9,9840	15,1540	26,1135	31,8504
260	10,0654	15,2539	26,2789	32,0543
300	10,1204	15,3222	26,3898	32,1911
400	10,1920	15,4090	26,5271	32,3608
500	10,1987	15,4330	26,5636	32,4071
600	10,1472	15,3239	26,4025	32,2224
700	10,1440	15,2756	26,3147	32,1215

Table 6.6: Value of the flow rate in the jumper for water displacing oil changing pressure boost

From the graphs in figure 6.9 and 6.10 it is possible to notice a small variation. The alternations are largest in the beginning (during the first 16 seconds), and then seem to stabilize as time goes.

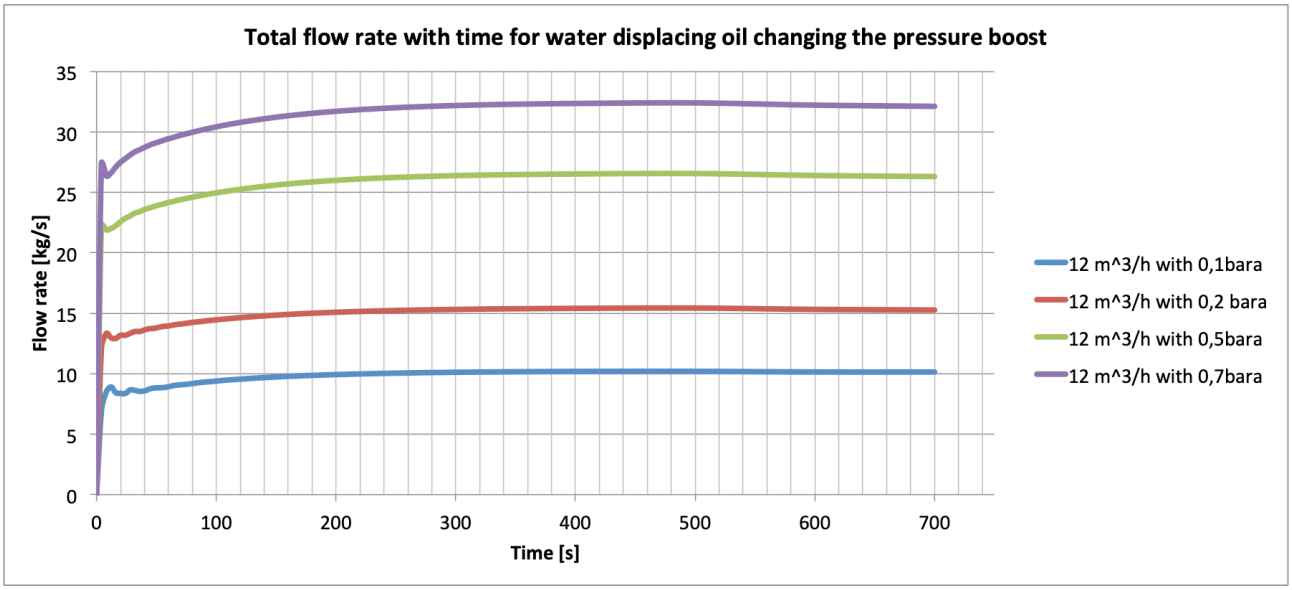

Figure 6.9: Flow rate with time changing the pressure boost

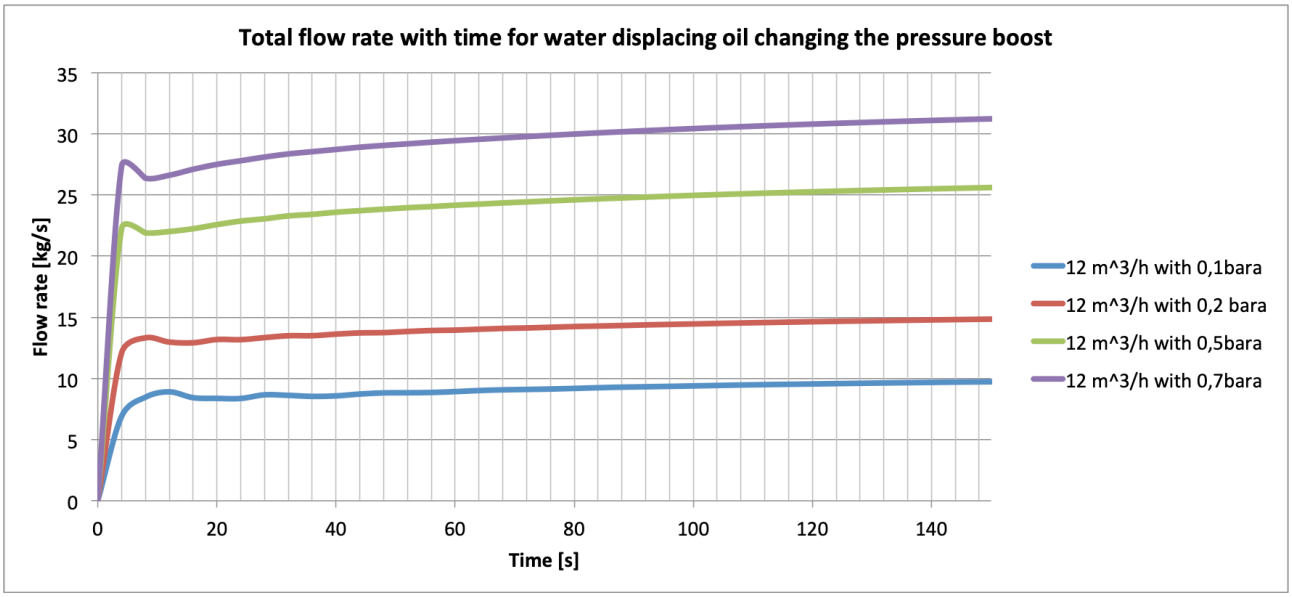

Figure 6.10: Details view of the first seconds of the chart in figure 6.9

6.3 Experiment results for water displacing oil

After having conducted the simulations exposed in the previous paragraph, it was possible to carry experiments in the Laboratory of the IGP Department of NTNU. This has been a great opportunity to validate and test the simulations through practical tests.

The following paragraph will hence expose the results of the experiments, conducted in the U-shaped jumper, taking into consideration the setup as described in section 4.3.2. It has to be clarified that the tests have been run only for water displacing oil considering three different injected flow rates and that the temperatures were measured during the experiments, given an average between 15 °C ± 0.2 °C, within a confidence interval of 95 %.

The results of the experiments where water is displacing oil are given in Table 6.7, and plotted in Figure 6.11.

Flow rate	Time	Oil VF
[m^3/h]	[s]	[-]
5 ± 0,70	50	88,83%
	100	68,25%
	150	36,13%
	250	16,10% ± 0,2%
	400	13,39% ± 0,2%
	700	12,36% ± 0,3%
10 ± 0,47	50	71,87%
	100	18,44% ± 0,2%
	150	12,20% ± 0,4%
	250	7,66% ± 0,4%
	400	6,43% ± 0,3%
	700	6,28% ± 0,4%
20,77± 0,46	50	17% ± 0,2%
	100	7% ± 0,3%
	150	0,067% ± 0,3%
	250	0,013% ± 0,3%
	400	0,001% ± 0,4%
	700	0%± 0,4%

Table 6.7: Results from experiment where water is displaced by oil

The oil volume fraction data shown in the table can be subject to error. In this case the error may be due to an incorrect reading of the height of the oil on the meter placed on the surface of the pipes. Also for the time was considered a possible error. It is possible to consider the case in which you want to stop the experiment exactly at 15 s, with a consequent reaction time roughly equal to 0.25 s, and the accuracy of the timer is 1e-3 s. Therefore, to report the error associated with time, you have to use the biggest one, i.e. 15 s +- 0.25 s.

Analysing the results obtained and shown by the chart in figure 6.11, it is possible to state that the trend of the oil volume fraction is similar to the trend obtained with the simulations carried out in LedaFlow. Increasing the initial flow rate, passing for example from 10 m^3/h to 20.77 m^3/h is easy to see from the graph that the time to remove the oil from the pipe decreases quickly.

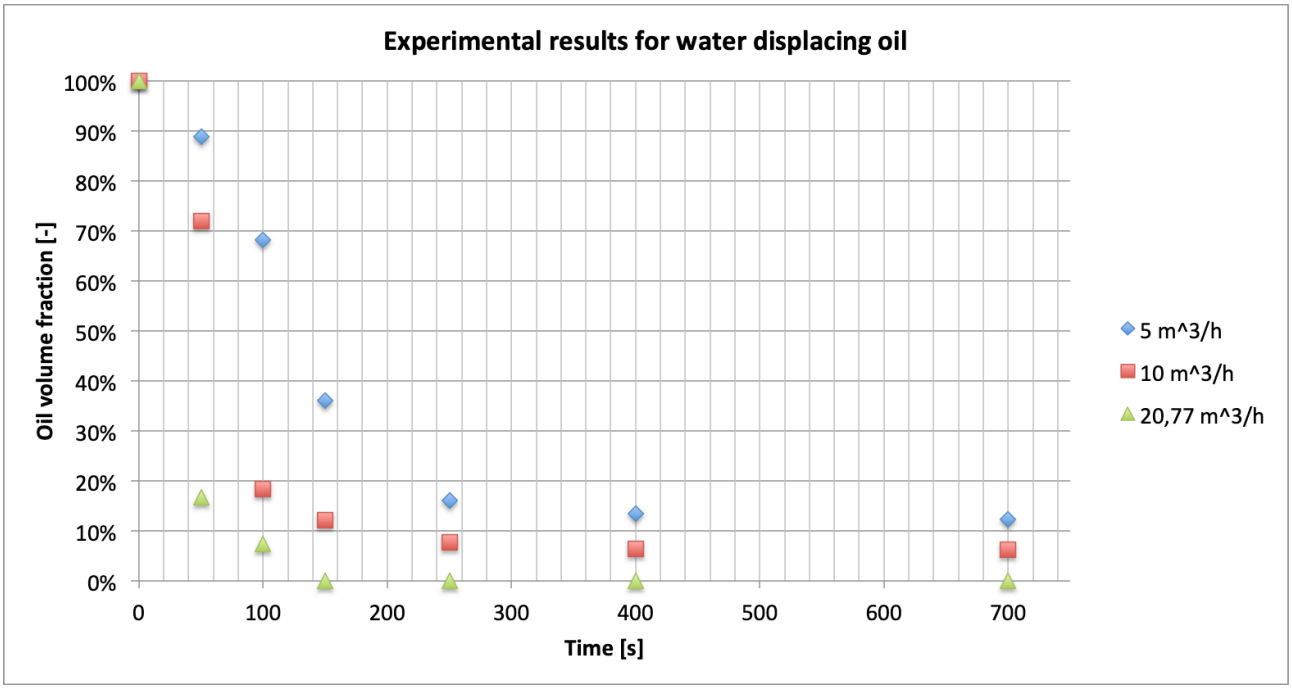

Figure 6.11: Experimental results for water displacing oil

The ideal situation would be to have, as quickly as possible, a value of less than 10% of oil volume fraction in the Jumper. During the experiments, imposing a flow rate equal to 5 m^3/h, after 700 seconds oil volume fraction values equal to about 12,36% were recorded; imposing an injected flow rate of 10m^3/h, instead, it is possible to arrive well below the desired threshold and a value of about 6,3 % of oil volume fraction were recorded, even if already after 250 seconds the oil volume fraction value is equal to 7,6%.

Increasing the injected flow rate up to 20,77 m^3/h, instead, it is possible to reach a smaller percentage of 10% of oil volume fraction already after 100s; after 700 seconds the jumper is

completely full of water and there are no more traces of oil, as it is possible to see from the photos in the figure 6.12 taken in the laboratory.

Figure 6.12: Pipes after 700 seconds injecting 20,77 m^3/h when water displacing oil

In order to understand what was the margin of error in the flow rate, which as explained in the chapter 4.3.2 was adjusted manually, an analysis through the data collected by the flow meter for all three cases studied were performed.

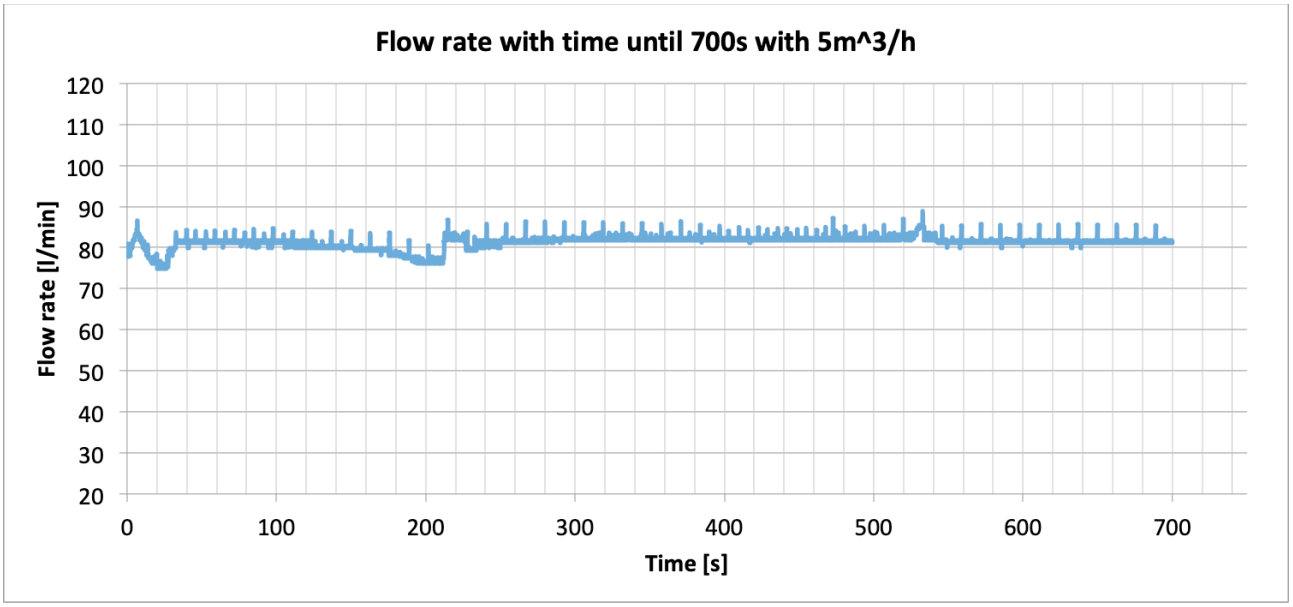

Figure 6.13: Experimental flow rate through the jumper for water displacing oil with 5m^3/h

Analysing the graphs in figure 6.13, 6.14 and 6.15, it can be state with good approximation that the greater uncertainty in the course of the flow occur during the first seconds. This is due to the fact that during this lapse of time, through the valve located after the centrifugal pump, the flow was adjusted until the desired values were reached. After the first few seconds, the flow still has peaks, but a more stable trend can be observed. Making an average of all the values of flow rate recorded during all the temporal steps in which the experiments have been executed, it has been possible to determine, as it can be observed in the table, the possible uncertainty that can be found in the flow rate.

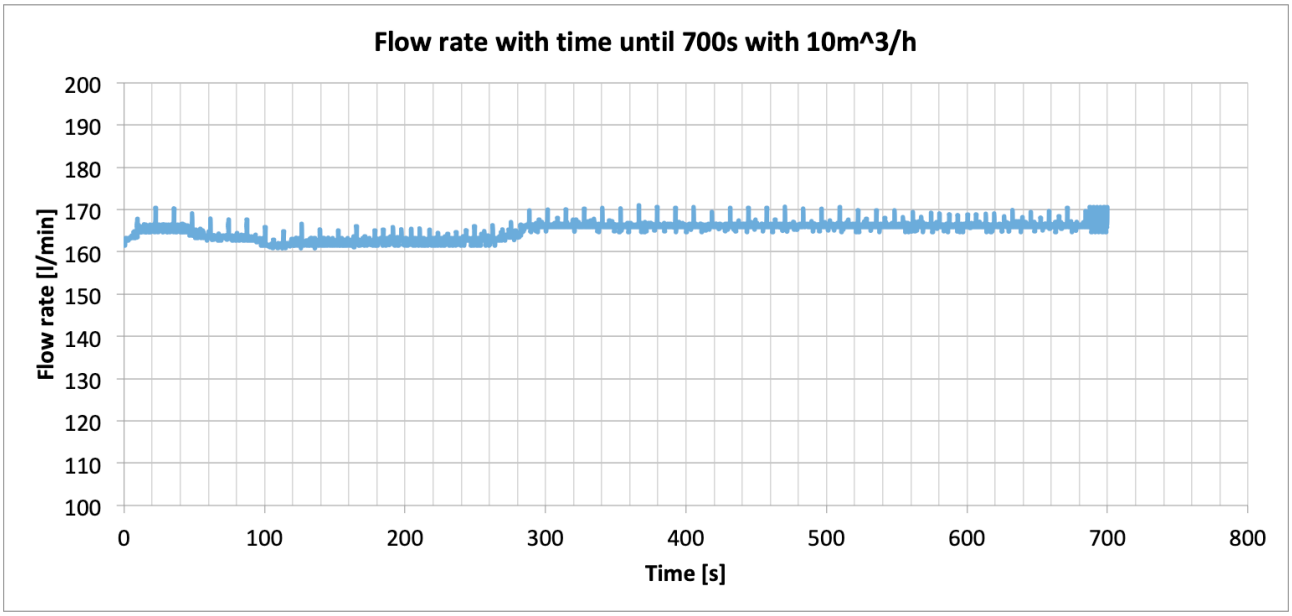

Figure 6.14: Experimental flow rate through the jumper for water displacing oil with 10m^3/h

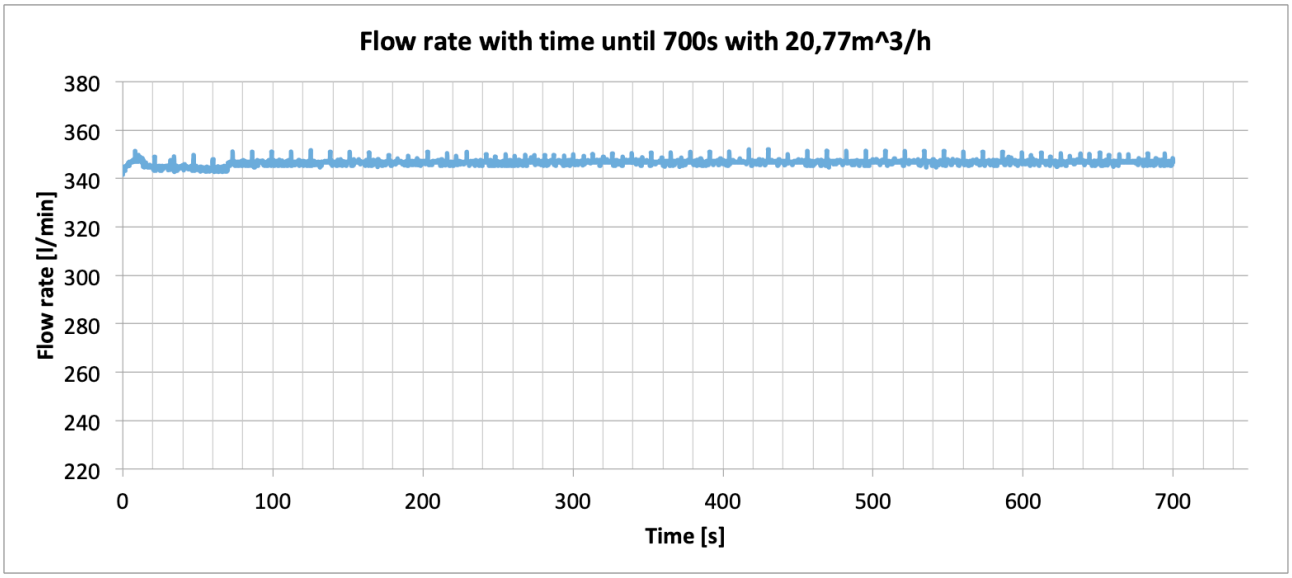

Figure 6.15: Experimental flow rate through the jumper for water displacing oil with 20,77m^3/h

Considering the case in which you have an injected flow rate of 5m^3/h, the uncertainty is equal to about 11.6 l/min, which is equivalent to about 0.70 m^3/h

For the case in figure 6.14, characterized by an injected flow rate equal to 10m3/h the oscillation has an average equal to approximately 7,83 l/min that correspond to 0,47 m^3/h. Analysing the last case, whose results are shown in the figure 6.15, the uncertainty is equal to about 7,67l/min equal to about 0,46 m^3/h.

6.4 Comparison of results

After having previously discussed the mathematical model and the LedaFlow results, it is now possible to compare these evidences with the results obtained in the laboratory, and assess the accuracy of the numerical model

For the first case of an injected flow rate of 5m^3/h, as it can be seen in the figure 6.16, the first two experimental data points show a greater presence of oil in the jumper compared to the three simulations. The three following data points between 150 seconds and 400 seconds, instead, seem to be close to the results of the mathematical model. The last value at 700 seconds is slightly different from the results obtained with the three models. The result obtained in the laboratory is greater than the mathematical model but less than the two models studied with LedaFlow.

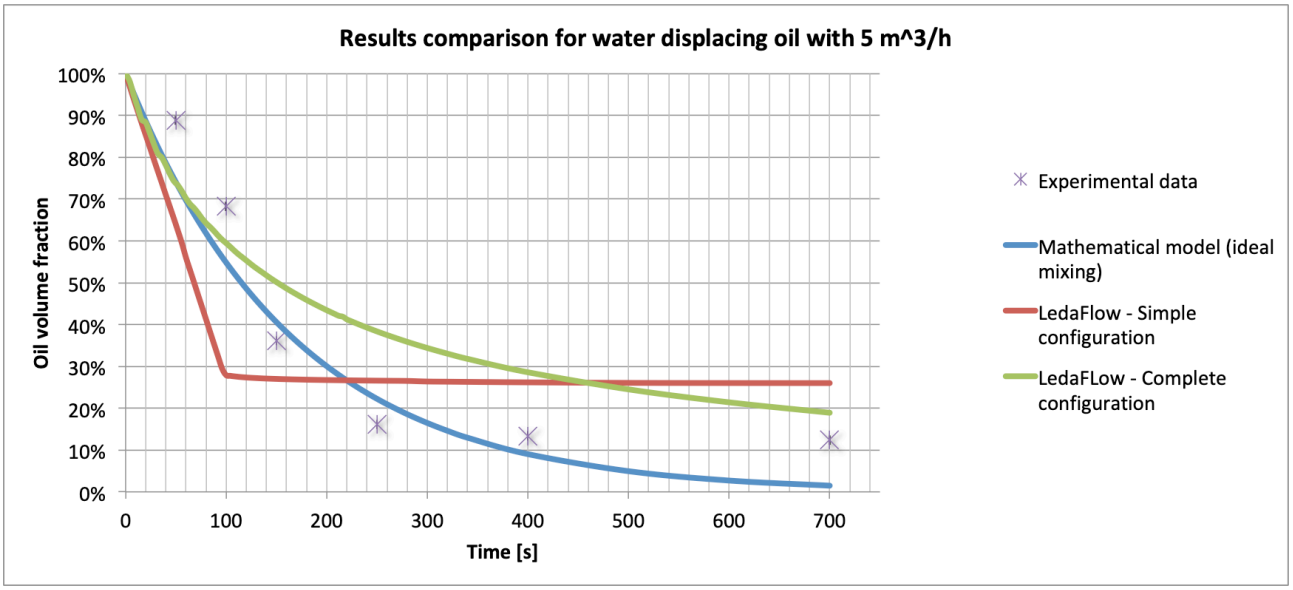

Figure 6.16: Comparison results for water displace oil with a flow rate of 5m^3/h

In order to show even more clearly the results obtained, a comparison was made between the complete configuration model created with LedaFlow and some photos taken in the laboratory. The figure 6.17 shows that also in this case the model made with LedaFlow overestimates the presence of oil inside the jumper compared to the experiments made in the laboratory. In the lower horizontal part of the jumper the model estimates a greater presence of oil than that photographed at the same time in the laboratory during the experiment.

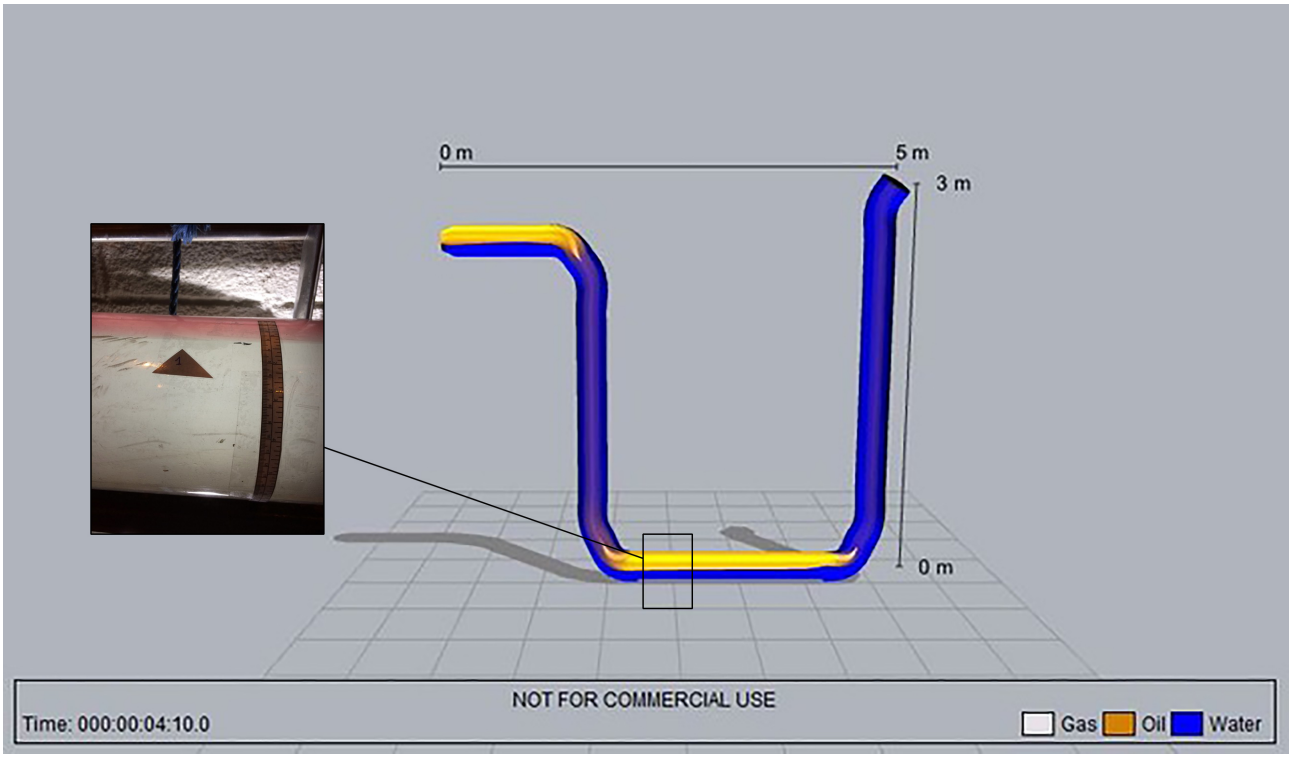

Figure 6.17: Comparison between the complete configuration and experimental results with a flow rate of 5 m^3/h

Also in the second case shown in the figure 6.18, which compares all the values obtained by imposing an initial flow rate of 10 m^3/h, the first data is overestimated the presence of oil inside the jumper compared to the other models. Data between 100 seconds and 250 seconds, on the other hand, are closer to the mathematical model and simple configuration created with LedaFlow.
Analysing the last two values obtained from laboratory experiments, we can state that they are very similar to the model characterized by the presence of the recirculation line (complex model).

The mathematical model underestimates the presence of oil inside the pipes as time goes, and at 700 seconds it is almost equal to 0. The simulations and the experiments carried out in the laboratory do not confirm such low values of oil volume fraction.

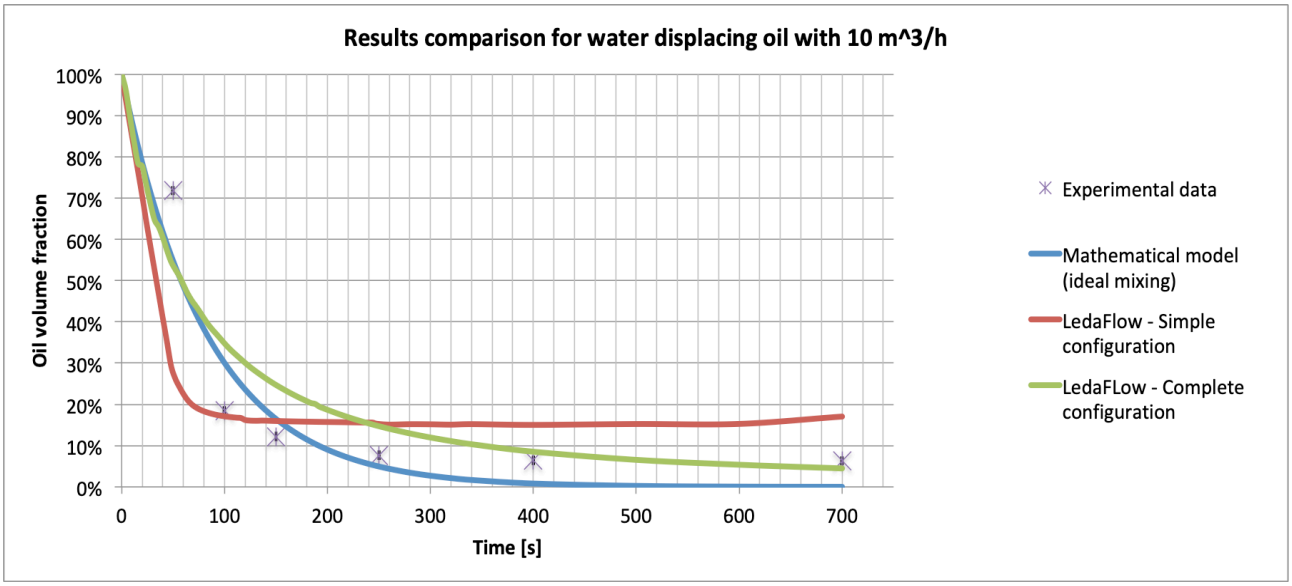

Figure 6.18: Comparison results for water displace oil with a flow rate of 10m^3/h

To confirm what is shown in the chart in figure 6.18, observing the figure 6.19 it is possible to see how the mathematical model overestimates the presence of oil inside the jumper. From the image taken during the experimentation phase, it can be seen that the presence of oil inside the jumper after 150 seconds is much lower than that estimated by the complete configuration model realized with LedaFlow simulator.

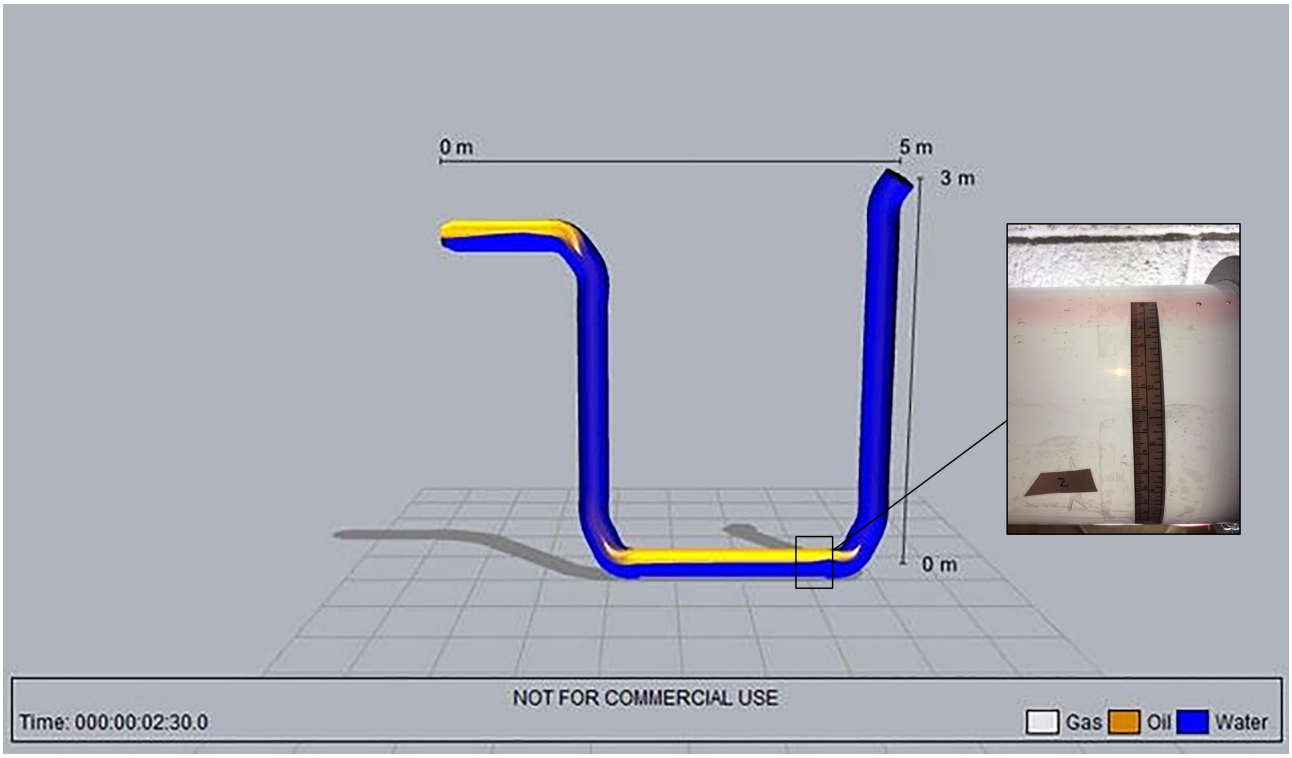

Figure 6.19: Comparison between the complete configuration and experimental results with a flow rate of 10 m^3/h

The last comparison is the one between all the simulations and the data from the laboratory for the case in which a flow rate equal to 20,77 m^3/h is injected.

It is possible to see that the first data found in the laboratory is probably a little closer to the data obtained with simple simulation. The other five data obtained from laboratory experiments, instead, seem to confirm almost perfectly the trend of the mathematical model and complex configuration.

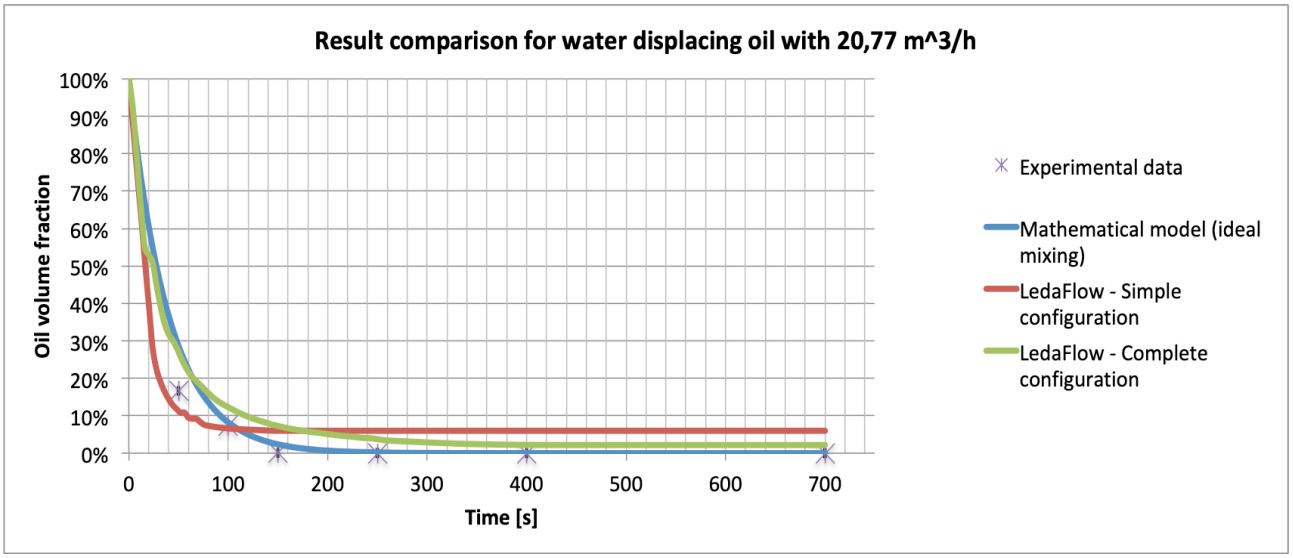

Figure 6.20: Comparison results for water displace oil with a flow rate of 20,77m^3/h

The amount of oil volume fraction estimated by the complete configuration with an injected flow rate of 20,77 m^3/h is closer to the results obtained in the laboratory, despite the image 6.21 shows that even in this case the results of oil volume fraction obtained with LedaFlow are higher than the actual amount of oil present during the experiments in the U-shaped jumper.

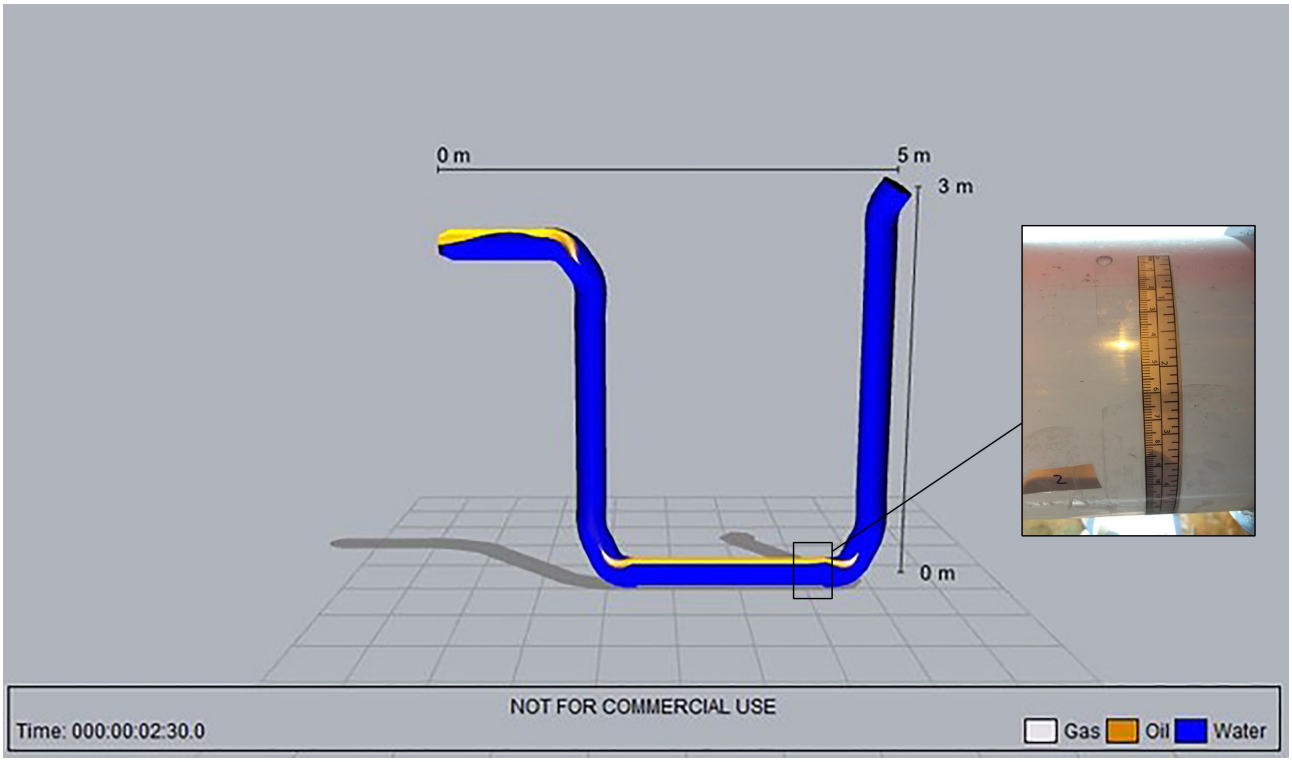

Figure 6.21: Comparison between the complete configuration and experimental results with a flow rate of 20,77m^3/h

Analyzing all three charts it can be stated that the simple configuration, in the final part of the simulation, tends to overestimate, compared to the other two models and the laboratory results, the presence of oil inside the jumper.

On the contrary, the mathematical model, at least for the first two cases, is underestimated, especially in the final part of the simulation, the presence of oil inside the jumper.

7. Conclusions

The displacement process of oil with water and water with oil in a U-shaped pipe geometry was reproduced experimentally and numerically with a commercial simulator and an ideal mixing model. The numerical results were in fair agreement with the experimental measurements.

According to the results of the numerical simulations, the flushing configuration without a recirculation line allows to flush faster the fluid initially present in the pipe, when compared against the configuration with the recirculation line. However, the amount of residual fluid in the jumper is highly dependent on the flushing flow rate. The configuration with the recirculation line allows to reach lower residual content of the initial fluid with lower injection rates.

According to numerical simulations of the configuration without recirculation line, a higher flushing flow rate is required when flushing water with oil than for flushing oil with water to achieve a low volume fraction of the initial fluid in the geometry.

Considering numerical simulations and experimental measurements of the configuration with recirculation line, the flow rate through the geometry in displacement process does not vary significantly during most of the displacement process.

Taking into account numerical simulations of the configuration with recirculation line, the magnitude of the flow rate through the geometry does not affect significantly the efficiency of the flushing process, within the ranges studied.

8. References

- Dr Najam Beg, Sacha Sarshar 2014. Surface Jet Pump (SJP) for Enhanced Oil & Gas Production. Caltec Edition.
- Exxol D60 Fluid Product Safety Sumary, ExxonMobil Chemicals. Available at: https://www.exxonmobilchemical.com/en/library/asset/80bd83e1923cfd9c85257762004897fb
- Falcone, G., Hewitt, G. F. and Almonti, C. (2009) *Multiphase Flow Metering*. Elsevier.
- Folde, H. G. 2017. Experimental and Numerical Study of Fluid Displacement in Subsea Pipe Sections. NTNU.
- GE Measurement and control (2011), UNIK5000 Pressure sensor platform. Available at: https://www.gemeasurement.com/sites/gemc.dev/files/unik_5000_series_datasheet_italiano.pdf
- GEA Liquid jet Liquid pump specification. Available at: https://www.gea.com/it/productgroups/pumps_valves/jet-pumps/index.jsp
- I.J. Karassic, J.P. Messina, P. Cooper, C.C. Heald, *Pump Handbook*, Fourth edition, McGraw-Hill, NY, 2008.
- J.Falcimaigne, S.Decarre, *Multiphase production, Pipeline Transport, Pumping and Metering*, IFP Publications, T Editions Technip.
- KONGSBERG 2015a. LedaFlow Advanced Transient Multiphase Flow Simulator.
- KONGSBERG (2015b) *LedaFlow user manual*.
- KONGSBERG 2016a. LedaFlow 2.0 - The Advanced Transient Multiphase Flow Simulator.
- KONGSBERG (2016b) 'LedaFlow Getting Started'.
- KONGSBERG Group, LedaFlow software, 2017. Available at: https://kongsberg.com/en/kongsberg-digital/oil%20and%20gas/flow%20assurance/ledaflow%20software%20-page/
- Lenntech, Centrifugal pump Grundfos CRNE15 – 04. Available at: https://www.lenntech.fr/grundfos/CRNE15/99071606/CRNE-15-4-A-FGJ-A-E-HQQE.html
- Nixon NT48-2" Turbine flow meter 110/1100 litres/min. Available at: https://nixon.stockshed.com/index.php?route=product/product&manufacturer_id=14&product_id=237&page=2
- Offshore (2016) *Subsea Production Systems Collection*. Tulsa: PennWell Corporation. Available at: https://www.offshore-mag.com/learning-center/subsea/subsea-processing-collection/subsea-processing-maps-and-posters.html

- Opstvedt, J. A. K. 2016. Experiments and Numeric Simulation on Displacement and Flushing of Hydrocarbon Fluid in Subsea Systems. NTNU.
- Society of Petroleum Engineering (SPE), Petrowiki, *Subsea process benefits.* Available at: https://petrowiki.org/Subsea_processing_benefits
- The Engineering Toolbox (2017) *Water – Thermodynamic Properties*. Available at: https://www.engineeringtoolbox.com/water-dynamic-kinematic-viscosity-d_596.html
- The Engineering Toolbox (2016f) *Thermoplastics - Physical Properties*. Available at: https://www.engineeringtoolbox.com/physical-properties-thermoplastics-d_808.html
- The Engineering Toolbox (2016e) *Thermal Expansion of PVC, CPVC, Carbon Steel, Stainless Steel and Fiberglass Pipes*. Available at: https://www.engineeringtoolbox.com/thermal-expansion-pvc-d_782.html
- http://www.ledaflow.com
- Yong Bai, Qiang Bai, *Subsea Engineering Handbook,* Elsevier, 2012.

9. Appendix

Appendix A: Method to build a model using LedaFlow simulator

In figure 9.1 it is possible to observe the starting graphical user interface for LedaFlow simulator.
The
The window is made up of a three different section. All saved cases can be found in the "case browser" window, they can be renamed and there is also an indication of the occupied MBs for each individual case. By clicking on the individual case, in this section you can also export the cases. With a "status window" is possible to see the progress of the running simulations. In this section of the software it is also possible to highlight any errors during the simulations.

The "display area" is the biggest one. Using this part of the window the operators from the toolbox are shown. The toolbox on the left side has five different functions highlighted in figure 9.2.

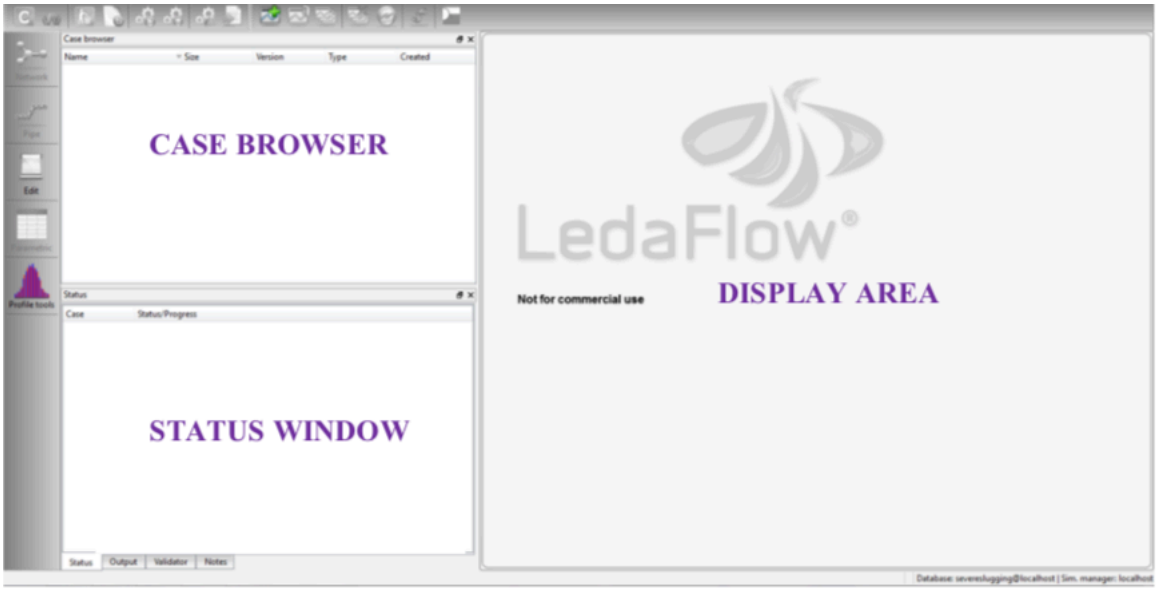

Figure 9.1: Graphical user interface LedaFlow

FUNCTION	Purpose
NETWORK	Visualization and constructing/editing the global networks: Where one can add pipes and components to a system
PIPE	Setting the geometry of the pipelines, the meshing and defining the wall properties
EDIT	Script functionalities
PARAMETRIC STUDY	Parametric study functionality
PROFILE TOOLS	Profile generation, filtering and simplification toll

Figure 9.2: Function of the toolbox (KONGSBERG, 2016b)

One of the first steps to start working on a new case is to right-click in the case browser window. At the beginning the user can choose between a default case of a simple case. The default case is characterized by the fact that it has 2 phases (liquid-gas) or 3 phases (water-oil-gas) that is composed of a 300-meter horizontal line with default properties.

In order to set a specific case simply clicks on the blue symbol highlighted in the figure 9.3.

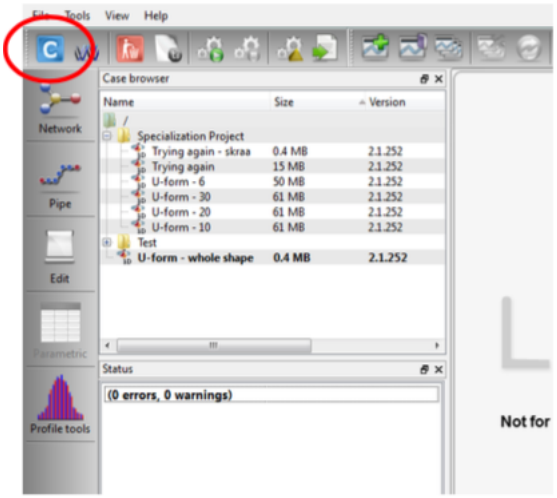

Figure 9.3: Graphical user interface LedaFlow

By clicking on the highlighted symbol, the window in figure 9.4 will appear, which is useful for setting the characteristic parameters such as temperature and pressure, thermal option and some other parameter useful to the simulation of flow assurance (emulsion, pigging, hydrate characteristics, etc.).

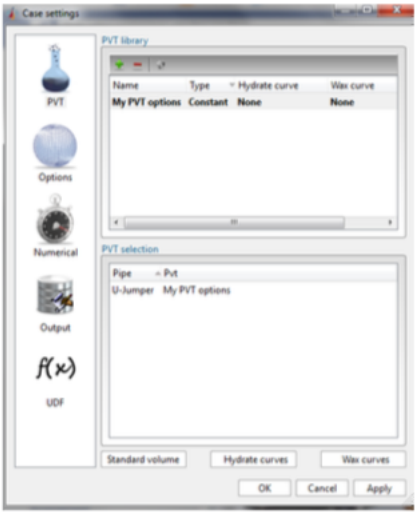

Figure 9.4: Graphical user interface to set characteristics parameters.

In this section is also possible to specify the numerical settings for the simulation. It is important to choose the simulation time (so the time the simulator will use to advance the solution) and the time step control, considering that LedaFlow is using dynamic time steps. The user may specify the maximum time step and the CFL number for a time period. The CFL number is the Courant-Friedrichs-Lewy condition number, and is specified to ensure that the time step is low enough in relation to the grid cell length and the phase velocities (KONGSBERG, 2016b).

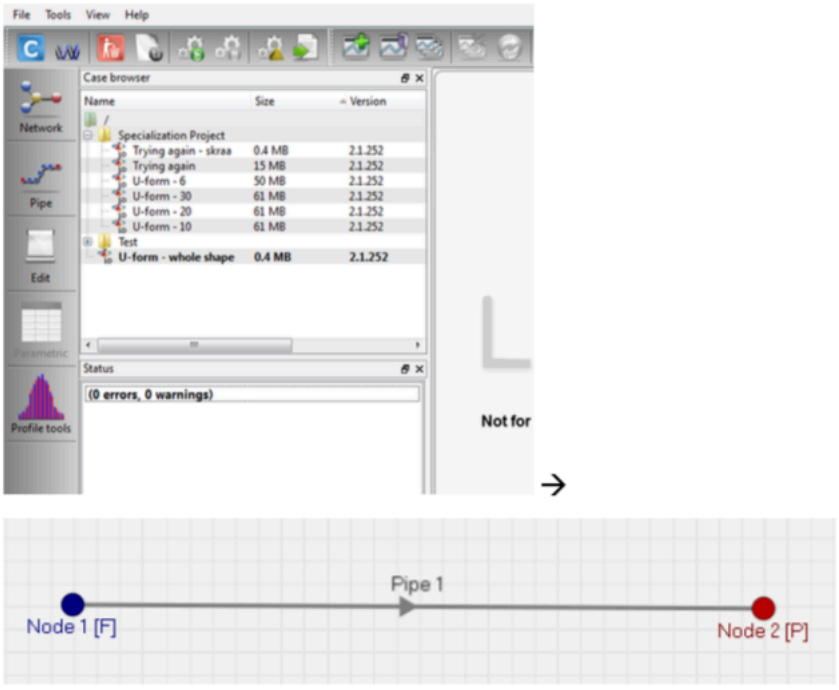

Figure 9.5: Graphical user interface to set characteristics parameters of the pipes.

Using the command “Network” it is possible to add extra pipelines to the system by right-clicking in the window or at the node where one wants the pipe to start/stop. Right-clicking on the pipeline it is also possible to add to the network extra devices such as valves, pumps, sources, separators, etc.

By clicking on the nodes it is possible to choose the boundary conditions choosing between either mass-pressure boundaries or pressure-pressure boundaries. In figure 9.6 and figure 9.7 different phase split options for the boundaries are listed.

Phase Split Options for Mass Inlet Boundary	
Flash	The mass fractions are calculated from the PVT table. Mass flowrates and fluid temperature need to be specified.
Flash hydrocarbons only	The mass fraction of gas and oil are calculated from PVT table but the mass fraction of water is specified by the user.
Mass fractions	The mass fractions of gas, oil and water have to be defined in addition to the total mass flow rate and the temperature of the fluid.
Standard volumes	The standard volume flowrate of gas or oil (optionally water too) and the fluid temperature need to be specified to calculate the mass flowrates of the phases based on flash calculations.

Figure 9.6: Phase Split options for mass inlet boundary (KONGSBERG, 2016b)

Phase Split Options for Pressure Boundary	
Flash	The volume fractions are calculated from PVT table. Pressure and fluid temperature need to be specified.
Flash hydrocarbons only	The mass fractions of gas and oil are calculated from PVT table but the mass fraction of water is specified by the user together with the pressure and fluid temperature.
Mass fractions Volume fractions	The mass or volume fractions of gas, oil and water should be specified. This option will be selected to account for back flow; for example if gas fraction is equal to 1, only gas will flow back.
Standard volume fractions	The user may provide 1 or 2 standard volume fractions. Instead of standard volume fractions, the user may provide GOR, GLR and WC but need to provide only 1 or 2 of them. The others are calculated automatically.

Figure 9.7: Phase Split options for pressure boundary (KONGSBERG, 2016b)

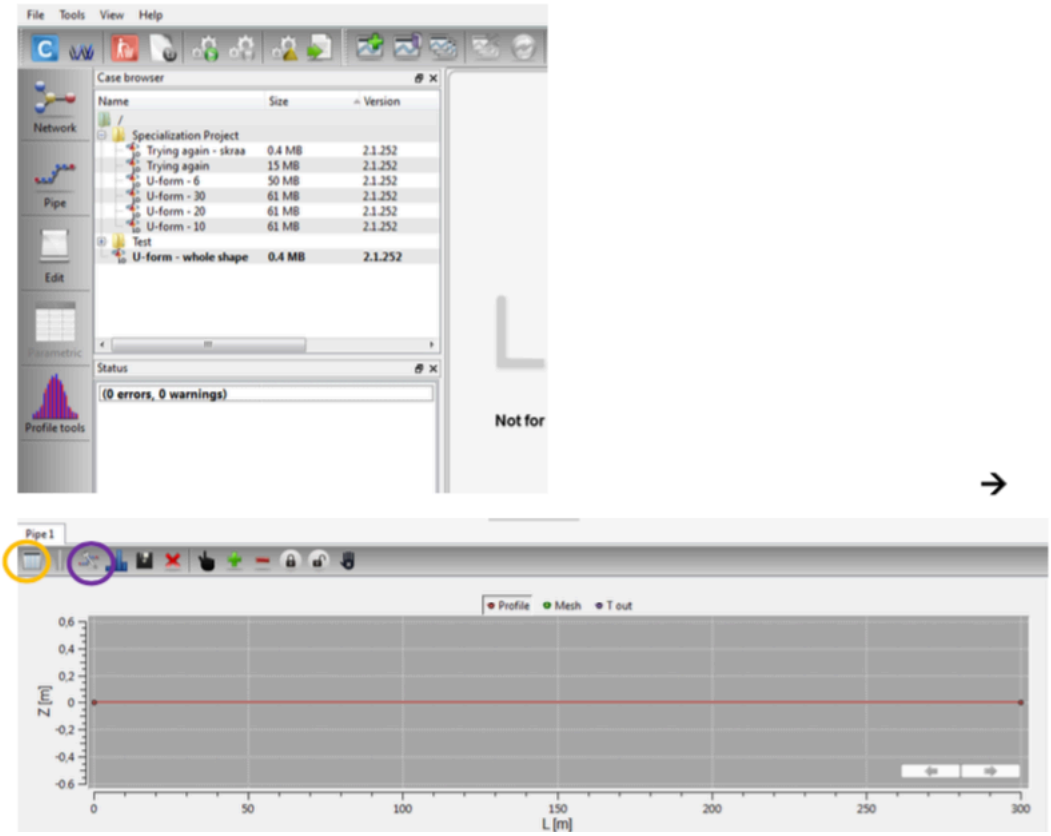

Figure 9.8: Graphical User Interface to set characteristics dimensions of the pipes

By clicking on pipe editor (orange circle) there are the possibilities to add or change properties of the pipelines. In this section is also possible to change the profile, adjust parameters related to the properties for thermal calculations and modify the geometry (diameter, roughness, wall type) of the pipeline.

With a purple circle is highlighted the mesh editor that allow to the user to add or change the mesh properties of the pipeline including adding or removing mesh points. The mesh is a discretization of the geometry used for numerical computation (KONGSBERG, 2016b).